Pizzio Bianchi, GA.; Rodriguez, L.; Antoni-Alandes, R.; Gonzalez Guzman, M.; Yunta, C.; Merilo, E.; Kollist, H.... (2013). The PYL4 A194T mutant uncovers a key role of PYL4-PP2CA interaction for ABA signaling and plant drought resistance. Plant Physiology. 163(1):441-455. doi:10.1104/pp.113.224162.

The PYL4 A194T mutant uncovers a key role of PYL4-PP2CA interaction for ABA signaling and plant drought resistance

Gaston A. Pizzio, Lesia Rodriguez, Regina Antoni, Miguel Gonzalez-Guzman, Cristina Yunta, Ebe Merilo, Hannes Kollist, Armando Albert and Pedro L. Rodriguez*

Instituto de Biologia Molecular y Celular de Plantas, Consejo Superior de Investigaciones Cientificas-Universidad Politecnica de Valencia, ES-46022 Valencia, Spain (G.A.P., L.R., R.A., M. G.-G., P.L.R.)

Institute of Technology, University of Tartu, Tartu 50411, Estonia (E.M., H.K.)

Departamento de Cristalografía y Biología Estructural, Instituto de Química Física Rocasolano, CSIC, ES-28006 Madrid, Spain (Y. C., A.A.)

One-sentence summary:

Enhanced drought resistance through mutagenesis of the PYL4 receptor that promotes enhanced interaction with PP2CA/AHG3

[1]This work was supported by the Ministerio de Ciencia e Innovacion, Fondo Europeo de Desarrollo Regional and Consejo Superior de Investigaciones Cientificas (grants BIO2011-23446 to P.L.R and BFU2011-25384 to A.A.; fellowships to R.A., L.R.; Juan de la Cierva contract to MGG) and by Estonian Ministry of Science and Education and European Regional Fund (IUT2-21 and Center of Excellence Environ to E.M. and H.K.).

*Corresponding author; e-mail prodriguez@ibmcp.upv.es

The author responsible for distribution of materials integral to the findings presented in this article in accordance with the Journal policy described in the Instructions for Authors (http://www.plantphysiol.org) is: Pedro L. Rodriguez (prodriguez@ibmcp.upv.es)

Abstract

Since ABA is recognized as the critical hormonal regulator of plant stress physiology, elucidating its signaling pathway has raised promise for application in agriculture, for instance through genetic engineering of ABA receptors. PYRABACTIN RESISTANCE1 (PYR1)/PYR1-LIKE (PYL)/ REGULATORY COMPONENTS OF ABA RECEPTORS (RCAR) ABA receptors interact with high affinity and inhibit clade A phosphatases type-2C (PP2Cs) in an ABA-dependent manner. We generated an allele library composed of 10000 mutant clones of *Arabidopsis thaliana* PYL4 and selected mutations that promoted ABA-independent interaction with PP2CA/ABA-HYPERSENSITIVE3 (AHG3). In vitro protein-protein interaction assays and size exclusion chromatography confirmed that $PYL4^{A194T}$ was able to form stable complexes with PP2CA in the absence of ABA, in contrast to PYL4. This interaction did not lead to significant inhibition of PP2CA in the absence of ABA; however, it improved ABA-dependent inhibition of PP2CA. As a result, 35S:$PYL4^{A194T}$ plants showed enhanced sensitivity to ABA-mediated inhibition of germination and seedling establishment compared to 35S:PYL4 plants. Additionally, at basal endogenous ABA levels, whole rosette gas-exchange measurements revealed reduced stomatal conductance (Gst) and enhanced water use efficiency (WUE) compared to non-transformed or 35S:PYL4 plants, and partial up-regulation of two ABA-responsive genes. Finally, 35S:$PYL4^{A194T}$ plants showed enhanced drought and dehydration resistance compared to non-transformed or 35S:PYL4 plants. Thus, we describe a novel approach to enhance plant drought resistance through allele library generation and engineering of a PYL4 mutation that enhances interaction with PP2CA.

Introduction

Abscisic acid (ABA) plays a critical role both for plant biotic and abiotic stress response (Cutler et al., 2010). Since ABA is recognized as the critical hormonal regulator of plant response to water stress, both the ABA biosynthetic and signaling pathways can be considered as potential targets to improve plant performance under drought. Thus, it has been demonstrated that transgenic plants producing high levels of ABA display improved growth under drought stress compared to wild type (Iuchi *et al.* 2001; Qin & Zeevaart 2002). Priming of ABA biosynthesis can be obtained by direct over-expression of 9-*cis*-epoxycarotenoid dioxygenase, a key enzyme in the biosynthetic pathway (Iuchi *et al.* 2001; Qin & Zeevaart 2002), or through the use of chemicals that accelerate ABA accumulation (Jakab et al., 2005). On the other hand, some examples are also known of *Arabidopsis* mutants (*era1*, *abh1*, *pp2c* combined mutants) affected in ABA signaling that show both an enhanced ABA response and drought resistant phenotypes (Pei et al., 1998; Hugouvieux et al., 2001; Saez et al., 2006). For instance, enhancement of abscisic acid sensitivity and reduction of water consumption has been achieved in *Arabidopsis* by combined inactivation of the protein phosphatases type 2C (PP2Cs) ABI1 and HAB1, leading to drought resistant plants (Saez et al., 2006). Enhancing ABA signaling through the recently discovered PYR/PYL ABA receptors is another promising approach to improve plant drought resistance, for instance through over-expression or generation of constitutively active (CA) receptors (Santiago et al., 2009a; Saavedra et al., 2010; Mosquna et al., 2011). However, pleiotropic effects due to sustained effects of high ABA levels or active ABA signaling might negatively affect plant growth, since abiotic stress responses divert resources required for normal growth. For instance, it was shown that vegetative expression of CA receptors was post-transcriptionally abolished in the case of PYL2 (Mosquna et al., 2011).

Recent studies reveal at least two subclasses of PYR/PYL receptors, including monomeric and dimeric PYLs (Dupeux et al., 2011a; Hao et al., 2011). The dimeric receptors (PYR1, PYL1, PYL2) show a higher K_d for ABA (>50 μM, lower affinity) than monomeric ones (~1 μM); however, in the presence of certain clade A protein phosphatases 2C (PP2Cs), both groups of receptors form ternary complexes with high affinity for ABA (K_d 30-60 nM) (Ma et al., 2009; Santiago et al., 2009a, b). A third subclass appears when we consider the trans-dimeric PYL3 receptor, which suffers a cis- to trans-dimer transition upon ligand binding to facilitate the subsequent

dissociation to monomer (Zhang et al., 2012). Dimeric receptors occlude their surface of interaction with the PP2C in the dimer, so they are strongly ABA-dependent for dissociation and adoption of a PP2C-binding conformation (Dupeux et al., 2011a). In vitro, monomeric ABA receptors are able to interact in the absence of ABA to some extent with the catalytic core of ABI1/ABI2/HAB1/PP2CA phosphatases, although less stable complexes are formed compared to ternary complexes with ABA (Dupeux et al., 2011a; Hao et al., 2011; Antoni et al., 2013). Boosting of such interaction might lead to faster association kinetics with PP2Cs or faster response to low-intermediate ABA levels. A sub-branch of clade A PP2Cs comprises Highly ABA-Induced (HAI) phosphatases that show a more restrictive pattern of interaction with PYR/PYLs compared to ABI1/ABI2/HAB1/PP2CA (Bhaskara et al., 2012).

Yeast two hybrid (Y2H) assays reveal both ABA-independent and -dependent interactions among PYR/PYLs and PP2Cs (Ma et al., 2009; Park et al., 2009; Santiago et al., 2009a). However, tandem affinity purification (TAP) of PYL8-interacting partners in planta was largely dependent on ABA in order to recover PYL8-PP2C complexes (Antoni et al., 2013). Y2H interactions of PYR/PYLs and PP2Cs that are dependent on exogenous ABA offer the possibility to set up screenings involving the generation of allele libraries and growth tests aimed to identify mutations that render ABA-independent interactions. Such mutations might lead in the plant cell to receptors that i) show enhanced association kinetics with PP2Cs by generating additional contact points, ii) interfere with PP2C function by steric hindrance or, iii) when several mutations are combined, to CA receptors that inhibit PP2Cs in the absence of ABA. The interaction in Y2H assays of PYL4 and PP2CA, two representative members of the PYR/PYL and clade A PP2C families, respectively, was shown to be ABA-dependent (Lackmann et al., 2011). PYL4 shows high expression levels in different tissues and its inactivation is required to generate strongly ABA-insensitive combined *pyr/pyl* mutants (Gonzalez-Guzman et al., 2012). PP2CA plays a critical role to regulate both seed and vegetative responses to ABA, and regulates stomatal aperture through interaction with the anion channel SLAC1 and the kinase SnRK2.6/OST1 (Kuhn et al., 2006; Yoshida et al., 2006; Lee et al., 2009). Therefore, PP2CA is a physiologically relevant target to design PYR/PYL receptors that show enhanced interaction with the phosphatase, affecting ABA signaling and plant stress response.

Through the generation of a PYL4 allele library and Y2H assays, we selected several PYL4 mutations enabling ABA-independent interaction with PP2CA in yeast. We focused our work on the PYL4^{A194T} protein, which interacted with PP2CA in the absence of ABA. This interaction led to a very modest inhibition of PP2CA in the absence of ABA (using pNPP as a phosphatase substrate); however, it improved ABA-dependent inhibition of PP2CA. As a result, upon over-expression of PYL4^{A194T}, we observed enhanced sensitivity to ABA compared to non-transformed or 35S:PYL4 plants both in seed and vegetative tissues. Moreover, 35S:PYL4^{A194T} transgenic plants showed enhanced drought resistance compared to non-transformed or 35S:PYL4 plants. In contrast, a previous attempt to express a mutagenized version of an ABA receptor failed to detect protein expression in vegetative tissue and therefore phenotype analysis could only be performed in seeds (Mosquna et al., 2011).

Results

Identification of PYL4 mutations that promote ABA-independent interaction with PP2CA in yeast

PYL4 interacts in an ABA-dependent manner with PP2CA in Y2H assays (Lackman et al., 2011; Fig. 1A). We conducted error-prone PCR mutagenesis of the PYL4 receptor and generated an allele library of approximately 10,000 clones in the pGBKT7 vector. The library was shuttled to yeast AH109 by co-transformation with pGAD7-PP2CA. Yeast transformants were pooled and clones able to grow in the absence of exogenous ABA in medium lacking histidine and adenine were selected. Yeast plasmids were extracted, sequenced and retransformed in yeast cells to recapitulate the phenotype. Thus, different mutations in the encoded PYL4 protein were identified that enabled constitutive interaction with PP2CA (Fig. 1, A and B). Through site-saturation mutagenesis of PYR1, Mosquna et al., (2011) identified mutations located in 10 different residues of the receptor that promoted PYR1-HAB1 interactions in the absence of ABA. These mutations were clustered in the receptor-phosphatase interaction surface, specifically in the gating loop of PYR1, its C-terminal α-helix and H60. The H60 of PYR1 is a hotspot for activating mutations, and for instance, the H60P substitution destabilizes the PYR1 dimer and increases its apparent ABA affinity, and both PYR1^{H60P} and PYR1^{H60R} bound HAB1 in the absence of ABA (Dupeux et al., 2011a; Mosquna et al., 2011). The H60 equivalent residue in PYL4 is H82, and

interestingly we found in our screening a PYL4^{H82R} mutation that resulted in ABA-independent interaction with PP2CA (Fig. 1A). The H82R mutation was found combined with V97A but the individual V97A mutation did not affect the interaction in the absence of ABA, although it increased yeast growth in the presence of ABA (Fig. 1A). Other mutations that enhanced the interaction of PYL4 and PP2CA in the absence of ABA were A194T and the double mutation F130Y C176R (Fig. 1, A and B). Both A194T and C176R mutations are located in the C-terminal helix of PYL4, which represented another hotspot for activating mutations in PYR1 since this α-helix forms part of the receptor-phosphatase binding interface (Mosquna et al., 2011). The interaction of the PP2C HAB1 with PYL4 was also found to be ABA-dependent in yeast (Lackman et al., 2011), so we decided to test whether the PYL4 described mutations affected the interaction with HAB1 in the absence of ABA. However, in contrast to their effect on the interaction with PP2CA, these mutant versions of PYL4 behaved mostly as PYL4 when assayed with HAB1 (Fig. 1A).

Effect of PYL4 mutations on PP2CA activity in vitro

Y2H assays reveal both ABA-independent and -dependent interactions among PYR/PYLs and PP2Cs; however, PYR/PYL receptors inhibit the activity of clade A PP2Cs mostly in an ABA-dependent manner (Park et al., 2009; Ma et al., 2009; Santiago et al., 2009; Fujii et al., 2009). Thus, an ABA-independent interaction in Y2H assay does not necessarily imply capacity to inhibit phosphatase activity in the absence of ABA. Indeed, although most of the monomeric PYR/PYL receptors show ABA-independent interaction with different PP2Cs in Y2H assay, effective phosphatase inhibition requires ABA, and for instance, the in vivo binding of PYL8 to five clade A PP2Cs was largely dependent on ABA (Park et al., 2009; Ma et al., 2009; Santiago et al., 2009; Antoni et al., 2013). Therefore, we tested whether these mutations affected actually the activity of two clade A PP2Cs, i.e. PP2CA and HAB1. Using p-nitrophenyl phosphate (pNPP) as a substrate, we could detect a small inhibitory effect (20%) of PYL4^{A194T} on the activity of PP2CA in the absence of ABA with respect to PYL4 (Fig. 2A). However, although the H82RV97A and F130Y C176R mutations promoted ABA-independent interactions in Y2H assay, they did not affect PP2CA activity in the absence of ABA. In the presence of 1 μM ABA, PYL4^{A194T} also showed a higher inhibition of PP2CA than PYL4 (Fig. 2A). The other mutations behaved similarly to PYL4 except F130Y C176R, which showed lower capacity to inhibit PP2CA in the

presence of ABA. PYL4 inhibited more efficiently HAB1 than PP2CA (IC50 of 0.25 and 1 μM, respectively), and all PYL4 mutants inhibited HAB1 similarly to PYL4 (Fig. 2B).

Although phosphatase activity is usually measured using small phosphorylated molecules such as pNPP or phosphopeptides, in vivo phosphatase activity is addressed against phosphorylated proteins and therefore could involve substrate-dependent effects. Therefore, we also performed in vitro reconstitution of the ABA signaling cascade and measured the capacity of PYL4^{A194T} or PYL4 to inhibit the dephosphorylation of several PP2CA targets, i.e. OST1/SnRK2.6, ΔC-ABF2 (residues 1-173) and ΔC-ABI5 (residues 1-200) transcription factors or N-terminal fragment (residues 1-186) of the anion channel SLAC1 (Fig. 2C). First a phosphorylation reaction was performed where OST1 was autophosphorylated in vitro and in turn it phosphorylated ΔC-ABF2, ΔC-ABI5 and SLAC1$^{1-186}$ proteins. Next, these proteins were used as substrates of PP2CA that was pre-incubated (or not) for 10 min with PYL4 or PYL4^{A194T} either in the absence or presence of 30 μM ABA. In the absence of ABA, we did not find significant differences among PYL4 and PYL4^{A194T}. In the presence of 30 μM ABA, PYL4^{A194T} inhibited better than PYL4 the dephosphorylation by PP2CA of ΔC-ABI5 and SLAC1$^{1-186}$, although it was not more effective than PYL4 to inhibit the dephosphorylation of ΔC-ABF2 (Fig. 2C). PYL4^{A194T} shows enhanced capacity to interact with PP2CA in the absence of ABA, probably because novel contact points are generated by the mutation. Therefore, we reasoned that this mutation might also lead to enhanced association kinetics in the presence of ABA, particularly at low ABA levels or low phosphatase:receptor ratios. We performed dephosphorylation assays at low ABA concentrations (0.1, 0.5 and 1 μM) and 1:1 phosphatase:receptor ratio (Fig. 2D). In the presence of 0.5-1 μM ABA, PYL4^{A194T} inhibited better (2-3 fold) than PYL4 the dephosphorylation of ΔC-ABF2, ΔC-ABI5 and SLAC1$^{1-186}$. Protection of OST1 phosphorylation was also improved by PYL4^{A194T} compared to PYL4 (Fig. 2D).

In vitro and in vivo interaction of PYL4^{A194T} and PP2CA

The phenotype described below for 35S: PYL4^{A194T} plants (see Figures 4 to 7) prompted us to further analyze the interaction between PYL4^{A194T} and PP2CA using in

vivo and in vitro protein-protein interaction tests. First, BiFC assays were used to analyze the interaction of PYL4 or PYL4^{A194T} and either PP2CA or HAB1 in tobacco cells (Fig. 3A). To this end, we performed transient expression of PP2CA-YFP^{N} and YFP^{C}-PYL4 in epidermal cells of *N. benthamiana* using Agroinfiltration. The nuclear interaction between PP2CA and PYL4 did not require the addition of exogenous ABA; endogenous ABA levels in tobacco cells after Agroinfiltration appear to be enough to promote such interaction. The sub-cellular localization of PP2CA was previously investigated by Antoni et al., (2012) using both transient expression of PP2CA-GFP in tobacco cells and biochemical fractionation of *Arabidopsis* transgenic lines that express HA-tagged PP2CA. We found that PP2CA was localized both to nucleus and cytosol, however PP2CA-GFP appears to be predominantly localized in the nucleus and presumably a higher concentration of the protein is found in this compartment (Figure 3A). Both RFP-PYL4 and RFP-A194T show a similar localization pattern each other (Figure 3A). Injection of ABA enhanced the relative fluorescence of the PP2CA-PYL4 complex and made evident additional interaction at the cytosol (Supplemental Fig. S2). PYL4^{A194T} was able to interact with PP2CA in the cytosol at endogenous ABA levels and the relative fluorescence emission was higher in the PYL4^{A194T}-PP2CA interaction compared to PYL4 (Fig. 3B). Therefore, our results suggest that A194T is able to interact in the cytosol with PP2CA at low ABA levels, whereas PYL4 is not. In the nucleus, the higher concentration of PP2CA-GFP probably facilitates the BiFC interaction. In contrast, the interaction of HAB1 and either PYL4 or PYL4^{A194T} did not differ significantly (Fig. 3A and B).

Finally we performed in vitro protein-protein interaction assays. Non-His tagged PYL4^{A194T} could be co-purified with 6His-ΔNPP2CA using Ni-affinity chromatography in the absence of ABA, in contrast to PYL4 (Fig. 3C). Size exclusion chromatography and SDS-PAGE analysis of the eluted fractions confirmed that both proteins formed a 1:1 complex in the absence of ABA (Fig. 3D). Finally, a pull-down assay showed that whereas the interaction of PYL4 and PP2CA was dependent on the addition of ABA, ABA-independent binding could be observed for PYL4^{A194T} and PP2CA (Fig. 3E). Therefore, both in vivo and in vitro assays show a differential interaction of PYL4^{A194T} and PP2CA with respect to PYL4.

Analysis of transgenic lines over-expressing PYL4 mutants

In order to study the putative effect of PYL4 mutations on ABA signaling in vivo, we generated transgenic plants that over-expressed hemmaglutinin (HA)-tagged versions of PYL4 or the mutant versions PYL4^{V97A}, PYL4^{A194T}, PYL4$^{C176R\ F130Y}$ and PYL4$^{H82R\ V97A}$. Expression of the proteins in vegetative tissue was detected by immunoblot analysis and transgenic lines that expressed similar levels of PYL4 and mutant PYL4 proteins were selected for further analysis; however, PYL4$^{H82R\ V97A}$ lines consistently showed lower expression of the transgene compared to PYL4 or other mutant proteins (Fig. 4A). Over-expression of PYL4 or PYL4^{V97A} enhanced ABA-mediated inhibition of seedling establishment compared to non-transformed plants, whereas ABA sensitivity of PYL4$^{C176R\ F130Y}$ over-expressing (OE) plants was similar to non-transformed plants. Interestingly, both PYL4^{A194T} and PYL4^{H82RV97A} OE plants showed higher sensitivity to ABA-mediated inhibition of seedling establishment than PYL4 OE plants (Fig. 4B). Low concentrations of ABA (0.25-0.5 μM) delay seedling establishment of non-transformed Col wt and have a limited inhibitory effect on further growth of the seedlings (Fig. 4C). This effect was enhanced in PYL4 or PYL4^{V97A} OE plants, particularly evident at 0.5 μM ABA (Fig. 4C). In the case of PYL4^{A194T} and PYL4^{H82RV97A} OE plants, the effect was even visible at 0.25 μM ABA, indicating that these lines show higher sensitivity to ABA-mediated inhibition of shoot growth than PYL4 OE plants (Fig. 4C and 4D).

Subsequent generations of PYL4^{H82RV97A} transgenic plants showed reduced levels of the protein compared to homozygous T3 so we concentrated further analysis on PYL4^{A194T} transgenic lines, where expression of the transgene remained stable. Seed germination and seedling establishment analyses of PYL4^{A194T} OE lines confirmed the enhanced sensitivity to ABA observed in T3 seeds (Supplemental Fig. S1). Moreover, root and shoot growth analyses also revealed enhanced sensitivity to ABA in vegetative tissues (Fig. 5). We transferred 4-d-old seedlings to MS medium plates lacking or supplemented with 10 μM ABA and root growth was measured 10 d after transfer. Both PYL4 and PYL4^{A194T} OE plants showed enhanced ABA-mediated inhibition of root growth compared to non-transformed plants (Fig. 5, A and B). Shoot growth was evaluated by measuring the maximum rosette radius of plants grown for 11 d in MS medium lacking or supplemented with 10 μM ABA (Fig. 5C). Finally, we measured expression of two ABA-responsive genes, *RAB18* and *RD29B*, in mock- or 10 μM ABA-treated plants (Fig. 5D). In the absence of exogenous ABA treatment, expression

of *RAB18* and *RD29B* was 6- and 23-fold, respectively, up-regulated in PYL4^{A194T} OE plants compared to non-transformed plants. These results indicate a partial de-repression of ABA responsive genes in this line compared to non-transformed plants. However, after ABA-treatment, the induction of these genes was not higher than in non-transformed plants.

PYL4^{A194T} OE plants show enhanced water use efficiency and drought resistance

Regulation of stomatal aperture by ABA is a key adaptive response to cope with drought stress. In order to probe stomatal function in non-transformed Col, PYL4 and PYL4^{A194T} OE plants, we performed diurnal analysis of stomatal conductance (Gst) and transpiration in whole plants under basal conditions (Fig. 6A and B). Interestingly, both PYL4 and PYL4^{A194T} OE lines showed lower Gst and transpiration values than non-transformed Col plants during the day and night. Moreover, PYL4^{A194T} OE plants showed lower Gst values than PYL4 OE plants. Diurnal course of Gst was generally not affected in transformed plants; both OE lines closed their stomata like non-transformed Col wt during the night and showed maximum Gst values around mid-day, followed by pre-dark stomatal closure. Still, pre-dawn stomatal opening was more pronounced in non-transformed Col wt and PYL4 OE compared to PYL4^{A194T} OE plants. The latter result could be directly related to an enhanced ABA-sensitivity of PYL4^{A194T} OE plants, since diurnal stomatal movements are linked to ABA concentration via its effect on ion and sugar fluxes (Tallman, 2004).

The lower Gst values of PYL4 and PYL4^{A194T} OE plants suggest that under steady-state conditions, the stomata of PYL4 and PYL4^{A194T} OE plants have reduced aperture compared to non-transformed Col plants. Indeed, direct measurements of stomatal aperture using whole leaf imaging revealed that stomata of both PYL4 and particularly PYL4^{A194T} OE plants were more closed than those of non-transformed Col plants (Fig. 6C). Finally, we also performed water-loss assays of non-transformed Col, PYL4 and PYL4^{A194T} OE lines (Fig. 6D). Water-loss experiments were done using 15-d-old seedlings grown in a growth chamber, which were excised from Petri dishes and submitted to the drying atmosphere of a laminar flow hood (Fig. 6D). Water-loss kinetics indicated that PYL4^{A194T} OE lines lost less water than non-transformed or PYL4 OE lines (Fig. 6D). Finally, when scoring stomatal aperture, we noticed that stomatal density of PYL4 and PYL4^{A194T} OE lines was circa 10% lower than that of

non-transformed plants (Fig. 6E). Therefore, a partial explanation of the reduced water loss observed in these lines can be attributed to 10% reduced stomatal density. However, since stomatal density was similar in PYL4 and PYL4^{A194T} OE lines, but lower transpiration was found in PYL4^{A194T} compared to PYL4 OE lines, we conclude that A194T has a higher effect compared to PYL4.

Reduced net photosynthesis (Anet) could be a drawback caused by the reduced stomatal opening and Gst found in PYL4 and PYL4^{A194T} OE lines. Therefore, in order to evaluate the performance of these plants compared to non-transformed plants, we determined water-use efficiency (WUE), i.e. the amount of carbon gained per unit water lost, Anet/transpiration. Both PYL4 and PYL4^{A194T} OE lines showed a reduced Anet compared to non-transformed plants; however PYL4^{A194T} OE lines showed enhanced WUE compared to non-transformed and PYL4 OE plants because the strongly reduced transpiration compensated the effect on Anet (Figure 6E).

Finally, we performed drought resistance experiments under greenhouse conditions (Fig. 7). Plants were grown in a greenhouse under normal watering conditions for 15 d and then irrigation was stopped. This day was taken as 0-d, when average rosette radius did not differ significantly among non-transformed Col, PYL4 OE and PYL4^{A194T} OE plants (Fig. 7, A and B). However, we found that during the subsequent 5-d period, plant growth was reduced in non-transformed Col and PYL4 OE plants compared to PYL4^{A194T} OE plants (Fig. 7B). Severe wilting and yellowing of leaves were observed at 16-d in wt, in contrast to PYL4^{A194T} OE lines. Finally, at 19-d watering was resumed and survival of the plants was scored at 23-d. Col wt plants did not survive after drought stress, whereas around 30% and 60-70% of PYL4 and PYL4^{A194T} OE lines survived, respectively (Fig. 7C). Finally, since PYL4^{A194T} OE lines were hypersensitive to ABA and showed de-repression of ABA/drought responsive genes, we tested whether they showed enhanced survival after suffering severe dehydration in Petri dishes. These experiments were done using 15-d-old seedlings by submitting them to dehydration for 12 h in a laminar flow hood, followed by rehydration and scoring survival rate 3-d afterwards. Dehydration experiments revealed enhanced resistance of PYL4^{A194T} OE compared to PYL4 OE and non-transformed plants. Thus, approximately 40% of PYL4^{A194T} plants survived after 12 h of dehydration followed by rehydration (Fig. 7D).

Discussion

Under non-stress conditions, endogenous ABA levels play a critical role to regulate stomatal aperture, as revealed by the open stomata phenotype of multiple *pyr/pyl* mutants, and basal ABA signaling is also required for proper plant growth and root development (Barrero et al., 2005; Gonzalez-Guzman et al., 2012; Antoni et al., 2013; Merilo et al., 2013). On the other hand, plant response to drought is largely dependent on enhanced ABA biosynthesis and signaling in order to regulate both stomatal aperture and gene expression under water stress conditions (Cutler et al., 2010). Thus, some mutants or transgenic plants showing enhanced response to ABA also display enhanced drought resistance and reduced water consumption (Pei et al., 1998; Hugouvieux et al., 2001; Saez et al., 2006). In this work we describe a novel approach to confer drought resistance through genetic enginering of a mutated PYL4 receptor. The PYL4^{A194T} mutation here described cannot be considered a CA receptor, since we did not observe strong inhibition of PP2C activity in the absence of ABA. Indeed, triple and cuadruple combinations of mutations were required to obtain CA PYR1, PYL2 and PYL9 receptors, which showed full ABA-independent inhibition of HAB1, ABI1 and ABI2 (Mosquna et al., 2011). As a result, expression of a 35S:GFP-PYL2^{CA} transgene in *Arabidopsis* seeds activated ABA signaling even in the ABA-deficient *aba2-1* mutant (Mosquna et al., 2011). However, the existence of a post-transcriptional mechanism that abolished expression of PYL2^{CA} in vegetative tissue precluded further analysis and testing of drought resistance in adult plants (Mosquna et al., 2011). The PYL4^{A194T} mutation improved ABA-dependent inhibition of PP2CA and expression of the receptor could be detected in vegetative tissues of 35S:PYL4^{A194T} transgenic plants, which showed ABA hypersensitivity both in seed and vegetative responses. Moreover, 35S:PYL4^{A194T} exhibited enhanced drought resistance compared to non-transformed or 35S:PYL4 OE plants. Particularly interesting features were the partial de-repression of ABA responsive genes, reduced stomatal aperture and transpiration of these lines at basal endogenous ABA levels. Additionally, since PYL4^{A194T} showed enhanced capacity to inhibit PP2CA at low ABA levels, it is likely that 35S:PYL4^{A194T} plants are primed

for an accelerated response to stress conditions, which likely contributes to the enhanced drought resistance observed in these plants.

Y2H, in vitro protein-protein interaction and BiFC assays revealed that PYL4^{A194T} showed a distinct pattern of interaction with PP2CA with respect to PYL4 (Figures 1 and 3). Thus, both Y2H and pull-down assays indicated that PYL4^{A194T} interacted with PP2CA in the absence of ABA. BiFC assays showed enhanced interaction of PYL4^{A194T} and PP2CA compared to PYL4 at the endogenous ABA levels present in Agroinfiltrated tobacco cells. ABA-independent interaction in Y2H assay does not necessarily imply capacity to inhibit phosphatase activity in the absence of ABA (Park et al., 2009; Ma et al., 2009; Santiago et al., 2009; Fujii et al., 2009). Indeed, in the absence of ABA we only found a modest inhibitory effect of PYL4^{A194T} on PP2CA activity using pNPP but no significant effect when phosphorylated proteins were used as phosphatase substrate. In contrast, these substrates were better protected from PP2CA-mediated dephosphorylation by PYL4^{A194T} compared to PYL4 when ABA was present. It is likely that PYL4^{A194T} displays enhanced association kinetics with PP2CA than PYL4, particularly at low-intermediate levels of ABA, leading to enhanced formation of ternary complexes. Thus, PYL4^{A194T} might act at endogenous ABA levels or prime ABA-dependent interaction with PP2CA to speed initial response to stress. Additionally, the PYL4^{A194T}-PP2CA interaction might lead to steric hindrance of phosphatase activity in vivo by restricting access to the substrates. Steric inhibition of kinase activity by catalytically inactive phosphatase is well known in the field of ABA signaling (Lee et al., 2009; Soon et al., 2012). Thus, it was reported that an inactive form of PP2CA was able to inhibit SnRK2.6 kinase activity (Lee et al., 2009) and catalytically inactive HAB1 was still able to inhibit SnRK2.6 (Soon et al., 2012).

The effect of PYL4^{A194T} appeared to be specific for PP2CA with respect to HAB1, since it did not show a differential effect on HAB1 compared to PYL4. However, at this stage, we cannot exclude that other clade A phosphatases (for instance other members of the PP2CA branch) might also be differentially affected by PYL4^{A194T}. Alignment of clade A PP2Cs reveals two subgroups (the ABI1 and PP2CA branches) and subtle differences in some regions of the proteins that could affect the interaction with PYR/PYLs (Bhaskara et al., 2012; Santiago et al., 2012). For instance, Bhaskara et al., (2012) noticed that Highly ABA-Induce (HAI) PP2Cs showed a differential interaction with PYR/PYLs and marked preference for monomeric

receptors. Previous results revealed a certain specificity in the multiple interactions of the 9 clade A PP2Cs and 14 PYR/PYLs (Santiago et al., 2009; Szostkiewicz et al., 2009) and a differential inhibition of PP2CA by PYR/PYLs was recently reported (Antoni et al., 2012). Structural evidence for the PYL4^{A194T}-PP2CA complex is currently not available; however, taking as model other complexes can be observed a clear difference in the length of the α2β4 loop of clade A PP2Cs, which is close to the receptor-phosphatase binding interface (Fig. 8A and C). This α2β4 loop is clearly different in PP2CA/HAI PP2Cs compared to the ABI1 branch and it represents a potential point of interaction with PYL4^{A194T}. Additionally, the A194 residue is located at the C-terminal helix of PYL4, close to the receptor-phosphatase binding interface. Therefore, the A194T mutation might also indirectly influence the interaction of the C-terminal helix of PYL4 with PP2CA or establish new contact points with the α2β4 loop of certain clade A PP2Cs. Interestingly, PYL10, which shows ABA-independent inhibition of PP2CA (Hao et al., 2011), contains a threonine residue at the equivalent position of PYL4^{A194T} (Fig. 8B).

In summary, genetic engineering of ABA receptors might serve as a new tool to ameliorate drought stress either through the introduction of mutations in PYR/PYL genes that generate CA receptors (Mosquna et al., 2011), enhance ABA-dependent inhibition of PP2Cs or through the use of natural versions that enhance ABA-independent inhibition of PP2Cs (Hao et al., 2011). Expression driven by a strong constitutive promoter might lead to some pleiotropic effects that negatively affect growth or yield of crop plants. Such a drawback could be bypassed by introducing stress-inducible or tissue-specific promoters that would drive the expression of the receptor only under stress conditions or in certain tissues.

MATERIAL AND METHODS

Plant material and growth conditions

Arabidopsis thaliana plants were routinely grown under greenhouse conditions (40-50% relative humidity) in pots containing a 1:3 vermiculite-soil mixture. For plants grown under growth chamber conditions, seeds were surface sterilized by treatment with 70% ethanol for 20 min, followed by commercial bleach (2.5 % sodium hypochlorite)

containing 0.05 % Triton X-100 for 10 min, and finally, four washes with sterile distilled water. Stratification of the seeds was conducted in the dark at 4ºC for 3 days. Seeds were sowed on Murashige-Skoog (MS) plates composed of MS basal salts, 0.1% 2-[N-morpholino]ethanesulfonic acid, 1% sucrose and 1% agar. The pH was adjusted to 5.7 with KOH before autoclaving. Plates were sealed and incubated in a controlled environment growth chamber at 22ºC under a 16 h light, 8 h dark photoperiod at 80-100 μE m^{-2} sec^{-1}.

Construction of a PYL4 mutant library and analysis of yeast two hybrid interaction with PP2CA

We conducted error-prone PCR mutagenesis by amplification of the PYL4 open reading frame using the following primers: FPYL4NcoI, 5´-GCAGCAGCCATGGTTGCCG TTCACCGTCCTTCT and RPYL4EcoRIstop: CGCACGAATTCACAGAGACA TCT TCTTCTT, and the following conditions: 2 mM dGTP, dCTP and dTTP, 0.5 mM dATP, 12 mM MgCl2 and Taq polymerase. The PCR product was *Nco*I-*Eco*RI doubly digested, cloned into the pGBKT7 vector and DH10B cells were transformed by electroporation. Thus, we generated an allele library in *E. coli* of approximately 10,000 PYL4 mutant clones. The sequencing of 50 clones revealed on average 1.7 non-silent mutations per clone in the PYL4 sequence (207 amino acids). The library was shuttled to yeast AH109 by co-transformation with pGAD7-PP2CA. Yeast transformants were pooled and clones able to grow in the absence of exogenous ABA in medium lacking histidine and adenine were selected. Yeast plasmids were extracted, sequenced and retransformed in yeast cells to recapitulate the phenotype. Protocols for yeast two-hybrid assays were similar to those described previously (Saez *et al.,* 2008).

BiFC assay in *N. benthamiana*

Experiments were performed basically as described by Voinnet et al., (2003). The different binary vectors described above where introduced into *Agrobacterium tumefaciens* C58C1 (pGV2260) (Deblaere et al., 1985) by electroporation and transformed cells were selected in LB plates supplemented with kanamycin (50 μg/ml). Then, they were grown in liquid LB medium to late exponential phase and cells were harvested by centrifugation and resuspended in 10 mM morpholinoethanesulphonic

(MES) acid-KOH pH 5.6 containing 10 mM MgCl2 and 150 mM acetosyringone to an OD600 nm of 1. These cells were mixed with an equal volume of *Agrobacterium* C58C1 (pCH32 35S:p19) expressing the silencing suppressor p19 of tomato bushy stunt virus (Voinnet et al., 2003) so that the final density of *Agrobacterium* solution was about 1. Bacteria were incubated for 3 h at room temperature and then injected into young fully expanded leaves of 4-week-old *N. benthamiana* plants. Leaves were examined after 3-4 days under a Leica TCS-SL confocal microscope and laser scanning confocal imaging system. Quantification of fluorescent protein signal was done as described (Gampala et al., 2007) using the National Institutes of Health (NIH) Image software ImageJ v1.37.

Constructs were done in pSPYNE-35S (Walter et al., 2004) as well as gateway vector pYFP^{C}43 (a derivative of pMDC43 where GFP is replaced by YFP^{C}, Belda-Palazon et al., 2012). The coding sequence of At2g38310 (PYL4) was cloned into the pENTR223.1-Sfi entry vector, kindly provided by ABRC (clone G12806). The coding sequence of PYL4^{A194T} was PCR amplified, cloned into the pCR8/GW/TOPO and verified by sequencing. Next, constructs containing PYL4 and PYL4^{A194T} were recombined by LR reaction into pYFP^{C}43 destination vector or into pH7WGR2 to generate RFP fusion proteins. The coding sequence of HAB1 and PP2CA was excised from a pCR8/GW/TOPO construct using a double digestion *Bam*HI-*Stu*I and subcloned into *Bam*HI-*Sma*I doubly digested pSPYNE-35S.

Protein expression and purification

For small scale protein purifications, *E. coli* BL21 (DE3) cells transformed with the corresponding constructs were grown in 100 ml of LB medium to an OD_{600} of 0.6-0.8. At this point 1 mM isopropyl-β-D-thiogalactoside (IPTG) was added and the cells were harvested after overnight incubation at 20ºC. Pellets were resuspended in lysis buffer (50mM Tris pH 7.5, 250mM KCl, 10% Glycerol, 1 mM β-mercaptoethanol) and lysed by sonication with a Branson Sonifier 250. The clear lysate obained after centrifugation was purified by Ni-affinity. A washing step was performed using 50mM Tris, 250 mM KCl, 20% Glycerol, 30 mM imidazole and 1 mM β-mercaptoethanol washing buffer, and finally the protein was eluted using 50mM Tris, 250 mM KCl, 20% Glycerol, 250 mM imidazole and 1mM β-mercaptoethanol elution buffer

For protein-protein interaction experiments, the pET28a_ΔNPP2CA, pETM11_PYL4wt and pETM11_PYL4^{A194T} plasmids were transformed into *E. coli* BL21 (DE3). A total of 8 ml of an overnight culture were sub-cultured into 800 ml fresh 2TY broth (16 g Bacto tryptone, 10 g yeast extract, 5 g NaCl per litre of solution) plus kanamycin (50 μg ml^{-1}). Protein expression was induced with 0.3 mM IPTG and the cells were harvested after overnight incubation at 20ºC. Pellets were resuspended in 25 mM TrisHCl pH 8.0, 50 mM NaCl, 50 mM imidazole, 5 mM β-mercaptoethanol and disrupted by sonication. After centrifugation (40 min, 40000 g) at 277 K, the clear supernatant was filtered (pore diameter 0.45 mm; Millipore Corporation, Bedford, MA, USA). The 6His-tagged proteins were purified using Ni-NTA Agarose (Qiagen) according to the manufacturer's instructions. The filtered supernatant was mixed with the previously equilibrated beads. After incubation, a washing step with ten volumes of 25 mM TrisHCl pH 8.0, 50 mM NaCl, 20mM imidazole, 5 mM β-mercaptoethanol buffer was performed followed by the elution from the Ni^{2+} resin in a buffer with 500 mM imidazole. Imidazole was removed using a PD-10 column (GE Healthcare) and the His-tag was cleaved using TEV protease.

Binding assay of 6His-ΔNPP2CA and PYL4

6His-ΔNPP2CA pellets were resuspended in 25 mM TrisHCl pH 8.0, 150 mM NaCl, 50mM imidazole, 5 mM β-mercaptoethanol, 5mM Mg2+, mixed with 8 mg of either pure non-tagged (through TEV cleavage) PYL4 or PYL4^{A194T} and disrupted by sonication. The crude extracts were treated as described above using His-Trap HP columns from GE Healthcare to the capture step according to the manufacturer's instructions. In all cases, the purified proteins were subjected to a size exclusion chromatography using a Superdex200 10/300 (Amersham Biosciences Limited, UK) to analyze the behavior in a gel filtration of each protein and to isolate the complex. In order to perform pull-down assays, 6His-ΔNPP2CA was purified, next immobilized on Ni-NTA agarose beads (Qiagen) and incubated with either pure non-tagged PYL4 or PYL4^{A194T}. The mix was swirled 30 min at 4 °C and incubated in the absence or presence of 100 μM ABA. After three washes, proteins were eluted by adding 500 mM imidazol and analyzed by SDS-PAGE.

PP2C and OST1 *in vitro* activity assays

Phosphatase activity was measured using as a substrate either pNPP or phosphorylated ΔC-ABF2, ΔC-ABI5 and SLAC1$^{1-186}$ proteins. For the pNPP substrate, assays were performed in a 100 µl solution containing 25 mM Tris-HCl pH 7.5, 2 mM $MnCl_2$ and 5mM pNPP. Assays contained 2 µM phosphatase (PP2CA or HAB1), 4 µM receptor and the indicated concentrations of ABA. Phosphatase activity was recorded with a ViktorX5 reader at 405nm every 60 seconds over 30 minutes and the activity obtained after 30 minutes is indicated in the graphics. In order to obtain phosphorylated ΔC-ABF2, ΔC-ABI5 and SLAC1$^{1-186}$ proteins, phosphorylation reactions were done using the OST1 kinase basically as described previously (Dupeux et al., 2011b). ΔC-ABF2 and SLAC1$^{1-186}$ N-terminal fragments were prepared as described (Antoni et al., 2012; Vahisalu et al., 2010). ΔC-ABI5 recombinant protein (amino acid residues 1-200, containing the C1, C2 and C3 target sites of ABA-activated SnRK2s) was expressed in the pETM11 vector as described above. The reaction mixture containing the OST1 kinase and either ΔC-ABF2, ΔC-ABI5 or SLAC1$^{1-186}$ recombinant proteins was incubated for 50 min at room temperature in 30 µl of kinase buffer: 20 mM Tris-HCl pH 7.8, 20 mM $MgCl_2$, 2 mM $MnCl_2$, and 3.5 µCi of γ-^{32}ATP (3000 Ci/mmol). Thus, OST1 was autophosphorylated and in turn it phosphorylated ΔC-ABF2, ΔC-ABI5 and SLAC1$^{1-186}$ proteins. Next, they were used as substrates of PP2CA that was preincubated (or not) for 10 with PYL4 or PYL4^{A194T} either in the absence or presence of the indicated ABA concentration. The reaction was stopped by adding Laemmli buffer and the proteins were separated by SDS-PAGE using an 8% acrylamide gel and transferred to an Immobilon-P membrane (Millipore). Radioactivity was detected and quantified using a Phosphorimage system (FLA5100, Fujifilm). After scanning, the same membrane was used for Ponceau staining. The data presented are averages of at least three independent experiments.

Generation of transgenic lines

PYL4 or PYL4 mutants were cloned into pCR8/GW/TOPO entry vector (Invitrogen) and recombined by LR reaction into the gateway compatible ALLIGATOR2 vector (Bensmihen *et al.*, 2004). This construct drives expression of PYL4 under control of the

35S CaMV promoter and introduces a triple HA epitope at the N-terminus of the protein. Selection of transgenic lines is based on the visualization of GFP in seeds, whose expression is driven by the specific seed promoter At2S3. The ALLIGATOR2-35S:3HA-PYL4 or mutant constructs were transferred to *Agrobacterium tumefaciens* C58C1 (pGV2260) (Deblaere *et al.,* 1985) by electroporation and used to transform Columbia wild type plants by the floral dip method. T1 transgenic seeds were selected based on GFP visualization and sowed in soil to obtain the T2 generation. At least three independent transgenic lines were generated for each construct. Homozygous T3 progeny was used for further studies and expression of HA-tagged protein in 21-d-old seedlings was verified by immunoblot analysis using anti-HA-peroxidase (Roche).

Seed germination and seedling establishment assays.

After surface sterilization of the seeds, stratification was conducted in the dark at 4ºC for 3 d. Approximately 100 seeds of each genotype were sowed on MS plates supplemented with different ABA concentrations per experiment. To score seed germination, radical emergence was analyzed at 72 h after sowing. Seedling establishment was scored as the percentage of seeds that developed green expanded cotyledons and the first pair of true leaves.

Root and shoot growth assays.

Seedlings were grown on vertically oriented MS plates for 4 to 5 days. Afterwards, 20 plants were transferred to new MS plates lacking or supplemented with the indicated concentrations of ABA. The plates were scanned on a flatbed scanner after 10-d to produce image files suitable for quantitative analysis of root growth using the NIH software ImageJ v1.37. As an indicator of shoot growth, the maximum rosette radius was measured**.**

RNA analyses

ABA treatment, RNA extraction and quantitative RT-PCR amplifications were performed as previously described (Saez *et al.,* 2004).

Whole-rosette stomatal conductance and transpiration measurements

The *Arabidopsis* whole-rosette gas-exchange measurement device, plant growth practice and custom written program to calculate transpiration and Gst for water vapour have been described previously (Kollist et al. 2007; Vahisalu et al., 2008). For gas-exchange experiments, 25-28-d-old plants (rosette area 6-18 cm2) were used. Until measurements, plants were grown in growth chambers (AR-66LX and AR-22L, Percival Scientific, IA, USA) at 12/12 photoperiod, 23/18ºC temperature, air relative humidity of 70-75% and 150 µmol m^{-2} s^{-1} light. During gas-exchange measurements, temperature, air relatively humidity, photoperiod and light in the cuvettes were kept as similar as possible to the values in growth chambers. Photographs of plants were taken before and after the experiment and rosette leaf area was calculated using the NIH software ImageJ 1.37v. Leaf area values for the intermediary experimental period were calculated using linear regression between starting and final leaf area.

Water-loss and stomatal aperture assays.

2-3 weeks-old seedlings grown in MS plates were used for water-loss assays. Four seedlings per genotype with similar growth, three independent experiments, were submitted to the drying atmosphere of a laminar flow hood. Kinetic analysis of water-loss was performed and represented as the percentage of initial fresh weight loss at each scored time point. Stomatal aperture measurements were done in leaves of 5-week-old plants grown under greenhouse conditions using whole leaf imaging (Chitrakar and Melotto, 2010). Staining of whole leaves with propidium iodide was conducted and the aperture of 30-40 stomata (ratio width/length, two independent experiments) was measured using a Leica TCS-SL confocal microscope.

Drought stress

Plants grown under greenhouse conditions (10 individuals per experiment, three independent experiments) were grown under normal watering conditions for 15 days and then subjected to drought stress by stopping irrigation during 20 days. Next, watering was resumed and survival rate was calculated after 3 days by counting the percentage of plants that had more than four green leaves. Photographs were taken at the start of the experiment (day 0), after 16 and 19 days of drought, and 3 days after re-watering. Quantification of shoot-growth was performed at 2, 5, 7 and 9 d after stopping irrigation (day 0) by measuring the maximum rosette radius of the plants.

Dehydration treatment

2-weeks-old seedlings grown in MS plates were used for these experiments. Twenty seedlings per genotype (two independent experiments) were submitted to the drying atmosphere of a laminar flow hood for 12 hours (25 ºC ± 1 ºC, 25% ± 2% relative humidity), then rehydrated with 25 ml of water. Survival percentage was scored 3 days after rehydration by counting the percentage of plants that had at least four green leaves.

Accession numbers

The *Arabidopsis* Genome Initiative locus identifiers for *PYL4* and *PP2CA* are *At2g38310* and *At3g11410*, respectively.

Supplemental material

The following supplemental material is available for this article online:

Supplemental Fig. S1. Enhanced sensitivity to ABA-mediated inhibition of germination and early seedling growth in T4 PYL4^{A194T} OE plants compared to non-transformed Col and PYL4 OE plants.

Supplemental Figure S2. ABA infiltration reveals BiFC interaction of PYL4 and PP2CA both at nucleus and cytosol.

LITERATURE CITED

Antoni R, Gonzalez-Guzman M, Rodriguez L, Rodrigues A, Pizzio GA, Rodriguez PL (2012) Selective Inhibition of Clade A Phosphatases Type 2C by PYR/PYL/RCAR Abscisic Acid Receptors. Plant Physiol **158:** 970-980

Antoni R, Gonzalez-Guzman M, Rodriguez L, Peirats-Llobet M, Pizzio GA, Fernandez MA, De Winne N, De Jaeger G, Dietrich D, Bennett MJ, Rodriguez PL (2013) PYRABACTIN RESISTANCE1-LIKE8 plays an important role for the regulation of abscisic acid signaling in root. Plant Physiol **161:** 931-941

Barrero JM, Piqueras P, Gonzalez-Guzman M, Serrano R, Rodriguez PL, Ponce MR, Micol JL (2005) A mutational analysis of the ABA1 gene of Arabidopsis thaliana highlights the involvement of ABA in vegetative development. J Exp Bot **56:** 2071-2083

Bhaskara GB, Nguyen TT, Verslues PE (2012) Unique drought resistance functions of the highly ABA-induced clade A protein phosphatase 2Cs. Plant Physiol **160:** 379-395

Belda-Palazon B, Ruiz L, Marti E, Tarraga S, Tiburcio AF, Culianez F, Farras R, Carrasco P, Ferrando A (2012) Aminopropyltransferases involved in polyamine biosynthesis localize preferentially in the nucleus of plant cells. PLoS One **7:** e46907

Bensmihen S, To A, Lambert G, Kroj T, Giraudat J, Parcy F (2004) Analysis of an activated ABI5 allele using a new selection method for transgenic Arabidopsis seeds. FEBS Lett **561:** 127-131

Chitrakar R, Melotto M (2010) Assessing stomatal response to live bacterial cells using whole leaf imaging. J Vis Exp

Cutler SR, Rodriguez PL, Finkelstein RR, Abrams SR (2010) Abscisic acid: emergence of a core signaling network. Annu Rev Plant Biol **61:** 651-679

Deblaere R, Bytebier B, De Greve H, Deboeck F, Schell J, Van Montagu M, Leemans J (1985) Efficient octopine Ti plasmid-derived vectors for Agrobacterium-mediated gene transfer to plants. Nucleic Acids Res **13:** 4777-4788

Dupeux F, Santiago J, Betz K, Twycross J, Park SY, Rodriguez L, Gonzalez-Guzman M, Jensen MR, Krasnogor N, Blackledge M, Holdsworth M, Cutler SR, Rodriguez PL, Marquez JA (2011a) A thermodynamic switch modulates abscisic acid receptor sensitivity. EMBO J **30:** 4171-4184

Dupeux F, Antoni R, Betz K, Santiago J, Gonzalez-Guzman M, Rodriguez L, Rubio S, Park SY, Cutler SR, Rodriguez PL, Marquez JA (2011b) Modulation of Abscisic Acid Signaling in Vivo by an Engineered Receptor-Insensitive Protein Phosphatase Type 2C Allele. Plant Physiol **156:** 106-116

Fujii H, Chinnusamy V, Rodrigues A, Rubio S, Antoni R, Park SY, Cutler SR, Sheen J, Rodriguez PL, Zhu JK (2009) In vitro reconstitution of an abscisic acid signalling pathway. Nature **462:** 660-664

Gampala SS, Kim TW, He JX, Tang W, Deng Z, Bai MY, Guan S, Lalonde S, Sun Y, Gendron JM, Chen H, Shibagaki N, Ferl RJ, Ehrhardt D, Chong K, Burlingame AL, Wang ZY (2007) An essential role for 14-3-3 proteins in brassinosteroid signal transduction in Arabidopsis. Dev Cell **13:** 177-189

Gonzalez-Guzman M, Pizzio GA, Antoni R, Vera-Sirera F, Merilo E, Bassel GW, Fernandez MA, Holdsworth MJ, Perez-Amador MA, Kollist H, Rodriguez PL (2012) Arabidopsis PYR/PYL/RCAR Receptors Play a Major Role in Quantitative Regulation of Stomatal Aperture and Transcriptional Response to Abscisic Acid. Plant Cell **24:** 2483-2496

Hao Q, Yin P, Li W, Wang L, Yan C, Lin Z, Wu JZ, Wang J, Yan SF, Yan N (2011) The Molecular Basis of ABA-Independent Inhibition of PP2Cs by a Subclass of PYL Proteins. Mol Cell **42:** 662-672

Hugouvieux V, Kwak JM, Schroeder JI (2001) An mRNA cap binding protein, ABH1, modulates early abscisic acid signal transduction in Arabidopsis. Cell **106:** 477-487

Iuchi S, Kobayashi M, Taji T, Naramoto M, Seki M, Kato T, Tabata S, Kakubari Y, Yamaguchi-Shinozaki K, Shinozaki K (2001) Regulation of drought tolerance by gene manipulation of 9-cis-epoxycarotenoid dioxygenase, a key enzyme in abscisic acid biosynthesis in Arabidopsis. Plant J **27:** 325-333

Jakab G, Ton J, Flors V, Zimmerli L, Metraux JP, Mauch-Mani B (2005) Enhancing Arabidopsis salt and drought stress tolerance by chemical priming for its abscisic acid responses. Plant Physiol **139:** 267-274

Kollist T, Moldau H, Rasulov B, Oja V, Ramma H, Huve K, Jaspers P, Kangasjarvi J, Kollist H (2007) A novel device detects a rapid ozone-induce transient stomatal closure in intact Arabidopsis and its absence in abi2 mutant. Physiol Plant **129:** 796-803

Kuhn JM, Boisson-Dernier A, Dizon MB, Maktabi MH, Schroeder JI (2006) The protein phosphatase AtPP2CA negatively regulates abscisic acid signal transduction in Arabidopsis, and effects of abh1 on AtPP2CA mRNA. Plant Physiol **140:** 127-139

Lackman P, Gonzalez-Guzman M, Tilleman S, Carqueijeiro I, Perez AC, Moses T, Seo M, Kanno Y, Hakkinen ST, Van Montagu MC, Thevelein JM, Maaheimo H, Oksman-Caldentey KM, Rodriguez PL, Rischer H, Goossens A (2011) Jasmonate signaling involves the abscisic acid receptor PYL4 to regulate metabolic reprogramming in Arabidopsis and tobacco. Proc Natl Acad Sci U S A **108:** 5891-5896

Lee SC, Lan W, Buchanan BB, Luan S (2009) A protein kinase-phosphatase pair interacts with an ion channel to regulate ABA signaling in plant guard cells. Proc Natl Acad Sci U S A **106:** 21419-21424

Ma Y, Szostkiewicz I, Korte A, Moes D, Yang Y, Christmann A, Grill E (2009) Regulators of PP2C Phosphatase Activity Function as Abscisic Acid Sensors. Science **324:** 1064-1068

Merilo E, Laanemets K, Hu H, Xue S, Jakobson L, Tulva I, Gonzalez-Guzman M, Rodriguez PL, Schroeder JI, Brosche M, Kollist H (2013) PYR/RCAR Receptors Contribute to Ozone-, Reduced Air Humidity-, Darkness- and CO2-Induced Stomatal Regulation. Plant Physiol May28

Mosquna A, Peterson FC, Park SY, Lozano-Juste J, Volkman BF, Cutler SR (2011) Potent and selective activation of abscisic acid receptors in vivo by mutational stabilization of their agonist-bound conformation. Proc Natl Acad Sci U S A **108:** 20838-20843

Pei ZM, Ghassemian M, Kwak CM, McCourt P, Schroeder JI (1998) Role of farnesyltransferase in ABA regulation of guard cell anion channels and plant water loss. Science **282:** 287-290

Qin X, Zeevaart JA (2002) Overexpression of a 9-cis-epoxycarotenoid dioxygenase gene in Nicotiana plumbaginifolia increases abscisic acid and phaseic acid levels and enhances drought tolerance. Plant Physiol **128:** 544-551

Saavedra X, Modrego A, Rodriguez D, Gonzalez-Garcia MP, Sanz L, Nicolas G, Lorenzo O (2010) The nuclear interactor PYL8/RCAR3 of Fagus sylvatica FsPP2C1 is a positive regulator of abscisic acid signaling in seeds and stress. Plant Physiol **152:** 133-150

Saez A, Apostolova N, Gonzalez-Guzman M, Gonzalez-Garcia MP, Nicolas C, Lorenzo O, Rodriguez PL (2004) Gain-of-function and loss-of-function phenotypes of the protein phosphatase 2C HAB1 reveal its role as a negative regulator of abscisic acid signalling. Plant J **37:** 354-369

Saez A, Robert N, Maktabi MH, Schroeder JI, Serrano R, Rodriguez PL (2006) Enhancement of abscisic acid sensitivity and reduction of water consumption in Arabidopsis by combined inactivation of the protein phosphatases type 2C ABI1 and HAB1. Plant Physiol **141:** 1389-1399

Saez A, Rodrigues A, Santiago J, Rubio S, Rodriguez PL (2008) HAB1-SWI3B interaction reveals a link between abscisic acid signaling and putative SWI/SNF chromatin-remodeling complexes in Arabidopsis. Plant Cell **20:** 2972-2988

Santiago J, Rodrigues A, Saez A, Rubio S, Antoni R, Dupeux F, Park SY, Marquez JA, Cutler SR, Rodriguez PL (2009a) Modulation of drought resistance by the abscisic acid receptor PYL5 through inhibition of clade A PP2Cs. Plant J **60:** 575-588

Santiago J, Dupeux F, Round A, Antoni R, Park SY, Jamin M, Cutler SR, Rodriguez PL, Marquez JA (2009b) The abscisic acid receptor PYR1 in complex with abscisic acid. Nature **462:** 665-668

Santiago J, Dupeux F, Betz K, Antoni R, Gonzalez-Guzman M, Rodrigues L, Marquez J, Rodriguez PL (2012) Structural insights into PYR/PYL/RCAR ABA receptors and PP2Cs. Plant Science **182:** 3-11.

Soon FF, Ng LM, Zhou XE, West GM, Kovach A, Tan MH, Suino-Powell KM, He Y, Xu Y, Chalmers MJ, Brunzelle JS, Zhang H, Yang H, Jiang H, Li J, Yong EL, Cutler S, Zhu JK, Griffin PR, Melcher K, Xu HE (2012) Molecular mimicry regulates ABA signaling by SnRK2 kinases and PP2C phosphatases. Science **335:** 85-88

Tallman G (2004) Are diurnal patterns of stomatal movement the result of alternating metabolism of endogenous guard cell ABA and accumulation of ABA delivered to the apoplast around guard cells by transpiration? J Exp Bot **55:** 1963-1976

Vahisalu T, Kollist H, Wang YF, Nishimura N, Chan WY, Valerio G, Lamminmaki A, Brosche M, Moldau H, Desikan R, Schroeder JI, Kangasjarvi J (2008) SLAC1 is required for plant guard cell S-type anion channel function in stomatal signalling. Nature **452:** 487-491

Vahisalu T, Puzorjova I, Brosche M, Valk E, Lepiku M, Moldau H, Pechter P, Wang YS, Lindgren O, Salojarvi J, Loog M, Kangasjarvi J, Kollist H (2010) Ozone-triggered rapid stomatal response involves the production of reactive oxygen species, and is controlled by SLAC1 and OST1. Plant J **62:** 442-453

Voinnet O, Rivas S, Mestre P, Baulcombe D (2003) An enhanced transient expression system in plants based on suppression of gene silencing by the p19 protein of tomato bushy stunt virus. Plant J **33:** 949-956

Walter M, Chaban C, Schutze K, Batistic O, Weckermann K, Nake C, Blazevic D, Grefen C, Schumacher K, Oecking C, Harter K, Kudla J (2004) Visualization of protein interactions in living plant cells using bimolecular fluorescence complementation. Plant J **40:** 428-438

Yoshida T, Nishimura N, Kitahata N, Kuromori T, Ito T, Asami T, Shinozaki K, Hirayama T (2006) ABA-hypersensitive germination3 encodes a protein phosphatase 2C (AtPP2CA) that strongly regulates abscisic acid signaling during germination among Arabidopsis protein phosphatase 2Cs. Plant Physiol **140:** 115-126

Zhang X, Zhang Q, Xin Q, Yu L, Wang Z, Wu W, Jiang L, Wang G, Tian W, Deng Z, Wang Y, Liu Z, Long J, Gong Z, Chen Z (2012) Complex structures of the abscisic acid receptor PYL3/RCAR13 reveal a unique regulatory mechanism. Structure **20:** 780-790

Fig. legends

Fig. 1. Identification of PYL4 mutations that generate ABA-independent interaction with PP2CA in a Y2H assay. A, Interaction of PYL4 or PYL4 mutants (baits, fused to the Gal4 binding domain) and either PP2CA or HAB1 (preys, fused to the Gal4 activating domain). Interaction was determined by growth assay on medium lacking His and Ade. When indicated, the medium was supplemented with 50 µM ABA. Dilutions (10^{-1}, 10^{-2}, 10^{-3}) of saturated cultures were spotted onto the plates and photographs were taken after 7 d. B, Alignment of PYR1 and PYL4 amino acid sequences and secondary structure. Location of the PYL4 mutations is marked by black asterisks. Red boxes indicate the position of the gate and latch loops. The green box indicates the position of the C-terminal α-helix. Red asterisks mark K59, E94, Y120, S122 and E141 residues of PYR1 involved in ABA binding.

Fig. 2. PYL4^{A194T} prevents better than PYL4 the PP2CA-mediated dephosphorylation of protein substrates in the presence of ABA. A, B, Phosphatase activity of either PP2CA or HAB1, respectively, was measured in vitro using p-nitrophenyl phosphate as a substrate in the absence or presence of PYL4 or different PYL4 mutant versions at the indicated ABA concentrations. Assays were performed in a 100 µl reaction volume that contained 2µM phosphatase and 4µM receptor. Data are averages ±SE from three independent experiments. * indicates $p<0.05$ (Student´s t test) when comparing data of mutant and wt PYL4 in the same assay conditions. C, D, Effect of PYL4^{A194T} or PYL4 on PP2CA-mediated dephosphorylation of OST1, ABF2 (1-173), ABI5 (1-200) and SLAC1 (1-186) phosphorylated proteins. C, The quantification of the autoradiography (numbers below) shows the percentage of protected phosphorylated substrate in each experiment relative to 100% in the absence of PP2CA. A 1:10 phosphatase:receptor stoichiometry was used in this assay. D, PYL4^{A194T} prevents better than PYL4 the PP2CA-mediated dephosphorylation of OST1, ABF2 (1-173), ABI5 (1-200) and SLAC1 (1-186). Value 1 expresses protection of each substrate in the absence of ABA and the normalized ratio expresses the fold number that either PYL4^{A194T} or PYL4 enhanced protection of the substrate at the indicated concentration of ABA. A 1:1 phosphatase:receptor stoichiometry was used in this assay.

Fig. 3. BiFC assay shows a different interaction of PYL4 or PYL4^{A194T} and PP2CA in tobacco leaves. PYL4^{A194T} binds ΔNPP2CA in the absence of ABA in vitro. A, Laser

scanning confocal imaging of epidermal leaf cells infiltrated with a mixture of *Agrobacterium* suspensions harboring the indicated BiFC constructs and the silencing suppressor p19. Right panels show the location of GFP and RFP fusions of PP2Cs and receptors, respectively. B, Quantification of the fluorescent protein signal. Images of panel A were analyzed using ImageJ software and signal intensity was calculated after subtracting the mean background density. C, SDS-PAGE showing the Ni2+ affinity chromatography purification from *E. coli* lysates containing recombinant 6His-ΔNPP2CA and either PYL4 (top) or PYL4^{A194T}(bottom). A lane showing PYL4 and PYL4^{A194T} is also displayed at the right of each gel. M, SF, FT and E1 to E4 stand for molecular mass markers, soluble fraction, flow through the column and eluted fractions at 500 mM imidazole, respectively. In the absence of ABA, PYL4^{A194T} co-purifies with 6His-ΔNPP2CA while PYL4 does not. D, Elution profiles after size exclusion chromatography in absence of ABA of pure PYL4^{A194T} (green), 6His-ΔNPP2CA (orange) and the eluted fractions described above containing the co-purified PYL4^{A194T}/6His-ΔNPP2CA (blue) proteins. Insets from each peak show SDS-PAGE analysis. The figure shows the formation of 1:1 PYL4^{A194T}:6His-ΔNPP2CA complex and the monomeric nature of PYL4^{A194T}. E, SDS-PAGE shows a pull-down assay where 6His-ΔNPP2CA is incubated with PYL4 or PYL4^{A194T} in absence or presence of 100 μM ABA.

Fig. 4. Enhanced sensitivity to ABA-mediated inhibition of seedling establishment and early seedling growth in PYL4 and PYL4^{A194T} OE lines compared to non-transformed Col plants. A, Immunoblot analysis using antibody against HA tag to quantify expression of PYL4, PYL4^{V97A}, PYL4^{A194T}, PYL4$^{C176R\ F130Y}$ and PYL4$^{H82R\ V97A}$ in 21-d-old seedlings of T3 transgenic lines (top). Ponceau staining is shown below. B, C, ABA-mediated inhibition of seedling establishment and early seedling growth in PYL4 and different PYL4^{mutant} OE lines compared to non-transformed Col plants. B, Approximately 100 seeds of each genotype (three independent experiments) were sown on MS plates lacking or supplemented with 0.25 or 0.5 μM ABA. Seedlings were scored for the presence of both green cotyledons and the first pair of true leaves after 8 d. Values are averages ± SE. C, Photographs of representative seedlings were taken 20 d after sowing. D, Quantification of ABA-mediated early seedling growth inhibition in

PYL4 and different PYL4^{mutant} OE lines compared to non-transformed Col plants. Data were obtained by measuring maximum rosette radius after 20 d and are averages ± SE from three independent experiments.

Fig. 5. Enhanced sensitivity to ABA-mediated inhibition of root growth of PYL4 and PYL4^{A194T} OE lines compared to non-transformed Col plants. A, Photographs of representative seedlings 10 d after the transfer of 4-d-old seedlings to MS plates lacking or supplemented with 10 µM ABA. B, C, Quantification of ABA-mediated root or shoot growth inhibition, respectively (values are means ±SE, growth of Col wt on MS medium was taken as 100%). * indicates $p<0.05$ (Student´s t test) when comparing data of PYL4 or PYL4^{A194T} OE plants to non-transformed Col plants in the same assay conditions. D, PYL4^{A194T} OE plants show partial constitutive up-regulation of ABA responsive genes in the absence of exogenous ABA. Expression of two ABA-inducible genes, *RAB18* and *RD29B*, in Col, PYL4 and PYL4^{A194T} OE plants was analyzed by quantitative RT-PCR in RNA samples of 2-week-old seedlings that were either mock or 10 µM ABA-treated for 3 h. Data indicate the expression level (values are means ±SE) of the *RAB18* and *RD29B* genes in each column with respect to mock-treated Col (value 1).

Fig. 6. Leaf gas-exchange measurements reveal reduced stomatal conductance and enhanced WUE in PYL4^{A194T} OE plants compared to non-transformed Col and PYL4 OE plants. A, Gst and B, Transpiration values of non-transformed Col, PYL4 and PYL4^{A194T} OE plants. Plants were kept in custom-made whole-rosette gas exchange measurement device (see Kollist et al. 2007) and Gst and transpiration were followed during a diurnal light/dark cycle for 27 hr. Values are mean ±SE (n=5). White and black bars above represent light and dark periods, respectively. C, Reduced stomatal aperture of both PYL4 and PYL4^{A194T} OE lines compared to non-transformed Col plants. *indicates $p<0.05$ (Student´s t test) when comparing data of OE lines and non-transformed Col plants in the same assay conditions. D, Loss of fresh weight of 15-d-old plants submitted to the drying atmosphere of a laminar flow hood. E, Stomatal density is reduced in PYL4 and PYL4^{A194T} OE lines compared to non-transformed Col plants. F, WUE is enhanced in PYL4^{A194T} OE lines compared to PYL4 OE and non-transformed plants. The values of Anet and WUE are averages for the whole day/light period. The different letters denote significant differences ($p<0.05$, n=5, ANOVA and Fisher´s least significant difference test).

Fig. 7. PYL4^{A194T} OE plants show enhanced drought and dehydration resistance. A, Enhanced drought resistance of PYL4^{A194T} OE plants with respect to non-transformed Col or PYL4 OE plants. Two-week-old plants were deprived of water for 19 days and then re-watered. Photographs were taken at the start of the experiment (0-d), after 16 and 19 days of drought (16 d, 19 d) and 2 days after re-watering (21d from 0d). Shoot was cut to better show the effect of drought on rosette leaves. B, Quantification of shoot-growth (maximum rosette radius) of non-transformed Col, PYL4 and PYL4^{A194T} OE plants during the course of the experiment. Measurements were taken at different times (2, 5, 7 and 9 d) after the start of the experiment and values at 0 d were taken as 100%. Values are means ±SE (n=10). C, Survival percentage of non-transformed Col, PYL4 and PYL4^{A194T} OE plants 3 d after re-watering. Values are means ±SE from three independent experiments (n=10 each). D, PYL4^{A194T} OE plants show enhanced resistance to dehydration. 2-week-old plants grown on MS plates were dehydrated by opening the lid in a laminar flow hood for 12 hours (25 ºC ± 1 ºC, 25% ± 2% relative humidity), next rehydrated and survival was scored 3 d later.

Fig. 8. Modeling of PYL4^{A194T} and PYL4^{H82R} mutations based on the PYR1-ABA-HAB1 structure. A, Location on PYR1 of equivalent PYL4 A194T and H82R residues using structure of the PYR1 (green)-ABA-HAB1 (orange) complex (PDB code 3QN1). The variable α2-β4 loop of clade A PP2Cs is displayed as a yellow ribbon for HAB1. The equivalent α2-β4 loop from ABI1 (as deduced from the PYL1-ABA-ABI1 complex, PDB code 3KDJ) is displayed as a blue ribbon. B, The length of the α2β4 loop (black box) notably differs among clade A PP2Cs. PP2CA displays the longer α2β4 loop and residues of the loop that show high identity with HAI PP2Cs (HAI1, At5g59220; HAI2, At1g07430; HAI3, At2g29380) are highlighted in green. Amino acid residues of HAB1/ABI1 involved in the interaction with PYR/PYL receptors are marked as green dots. C, The location of the PYL4 A194 residue at the C-terminal α helix and equivalent threonine residue of monomeric receptors PYL5, PYL10 and PYL13 is highlighted.

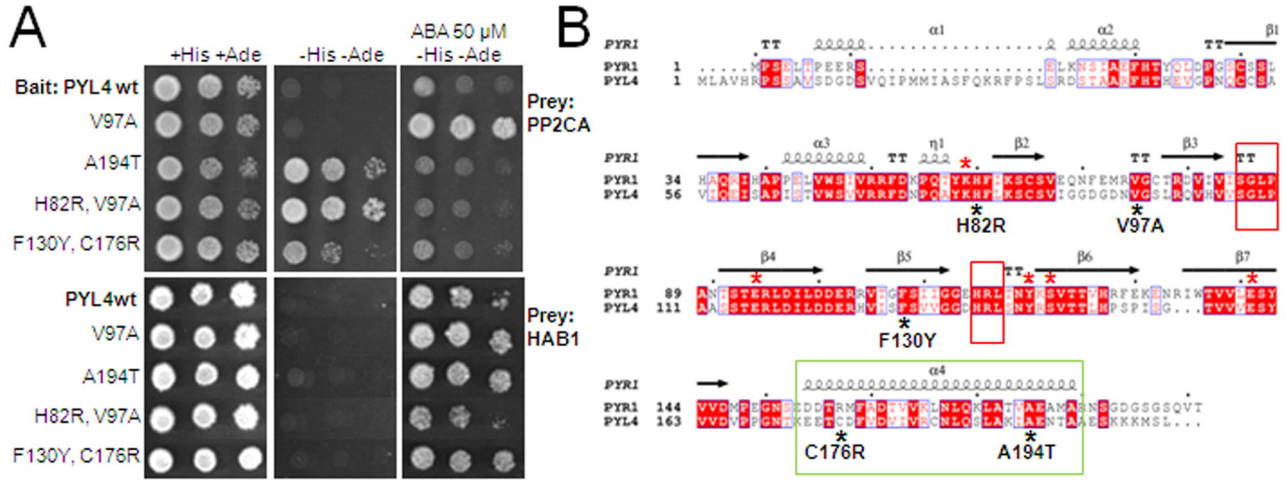
A
+His +Ade
-His -Ade
ABA 50 µM
-His -Ade
Bait: PYL4 wt
V97A
A194T
H82R, V97A
F130Y, C176R
Prey:
PP2CA
PYL4wt
V97A
A194T
H82R, V97A
F130Y, C176R
Prey:
HAB1
B
PYR1
PYR1 1 .....MPSEL
PYL4 1 MLAVHR
PSS
PEERS
CLKNSIAHFHT
α1
α2
β1
PYR1 34 HAQSIAPPFT
PYL4 56 VQSIAPTFT
VWSVVRRFDKPQAYKHFIKSCSV
IGGDGDNVGSIREVHVVSGLP
α3
η1
β2
β3
H82R
V97A
PYR1 89 ANISTERLDILDDER
PYL4 111 AASTERLDILDDER
RVGGFSIVGGEHRLVNYKSVTTLHPSPIGGTVVESY
β4
β5
β6
β7
F130Y
PYR1 144 VVDVMPQGNSEDTRMFADTVVKLNLQKLATIAEAMARNSGDGSGSQVT
PYL4 163 VVDVMPQGNKEETCVFVDNIVRCNLQSLAKHAENTAAESKKKMSL...
α4
C176R
A194T

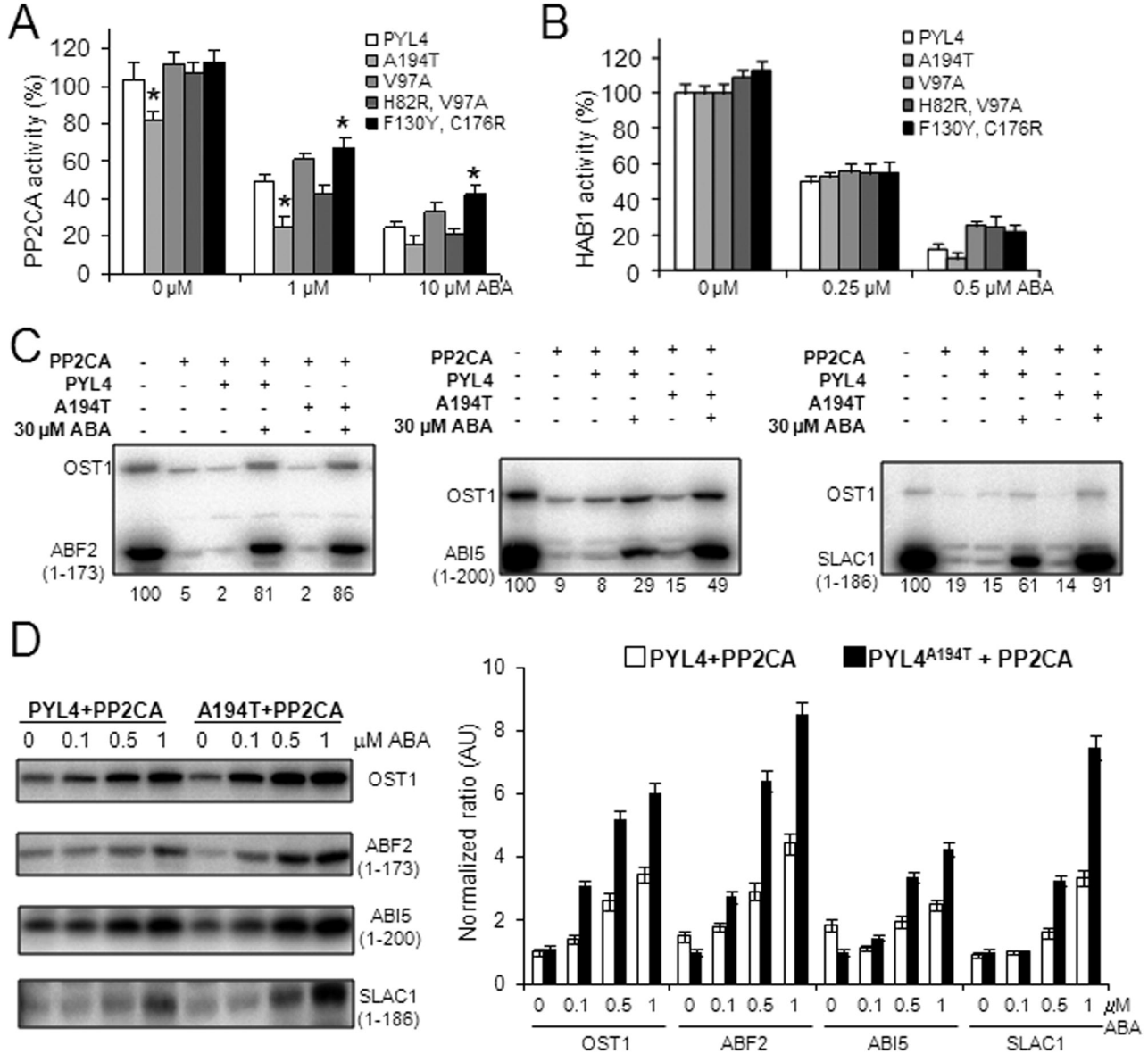
A
PP2CA activity (%)
PYL4
A194T
V97A
H82R, V97A
F130Y, C176R
0 μM
1 μM
10 μM ABA
B
HAB1 activity (%)
0 μM
0.25 μM
0.5 μM ABA
C
PP2CA
PYL4
A194T
30 μM ABA
OST1
ABF2 (1-173)
100 5 2 81 2 86
ABI5 (1-200)
100 9 8 29 15 49
SLAC1 (1-186)
100 19 15 61 14 91
D
PYL4+PP2CA
A194T+PP2CA
0 0.1 0.5 1 μM ABA
OST1
ABF2 (1-173)
ABI5 (1-200)
SLAC1 (1-186)
PYL4+PP2CA
PYL4A194T + PP2CA
Normalized ratio (AU)
0 0.1 0.5 1 μM ABA
OST1
ABF2
ABI5
SLAC1

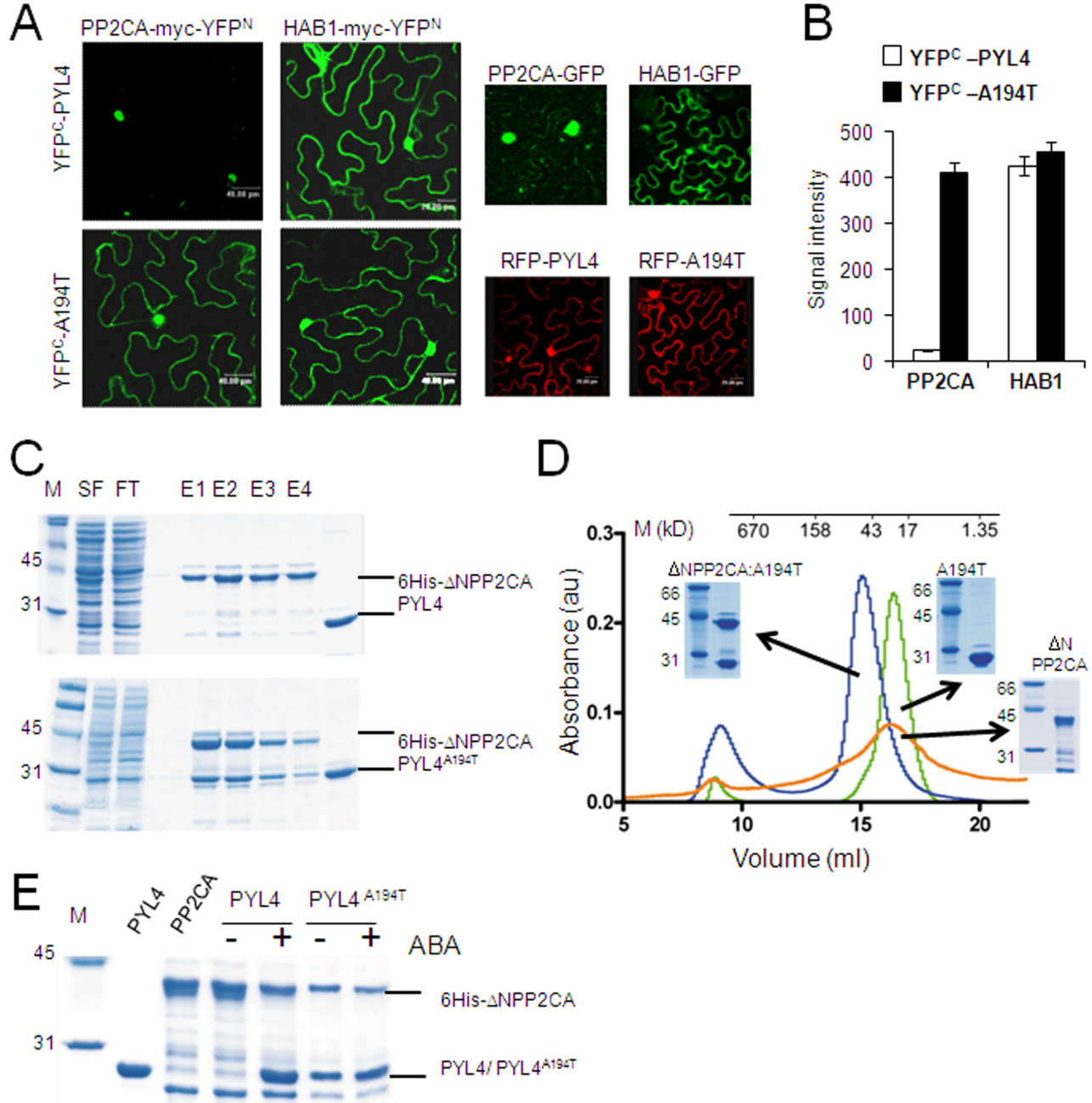
A
PP2CA-myc-YFP^N
HAB1-myc-YFP^N
YFP^C-PYL4
YFP^C-A194T
PP2CA-GFP
HAB1-GFP
RFP-PYL4
RFP-A194T
B
YFP^C –PYL4
YFP^C –A194T
Signal intensity
500
400
300
200
100
0
PP2CA
HAB1
C
M SF FT E1 E2 E3 E4
45
31
6His-ΔNPP2CA
PYL4
6His-ΔNPP2CA
PYL4^A194T
D
M (kD)
670 158 43 17 1.35
ΔNPP2CA:A194T
A194T
ΔN PP2CA
66
45
31
Absorbance (au)
0.3
0.2
0.1
0.0
5 10 15 20
Volume (ml)
E
M
PYL4
PP2CA
PYL4
PYL4 A194T
- + - +
ABA
45
31
6His-ΔNPP2CA
PYL4/ PYL4^A194T

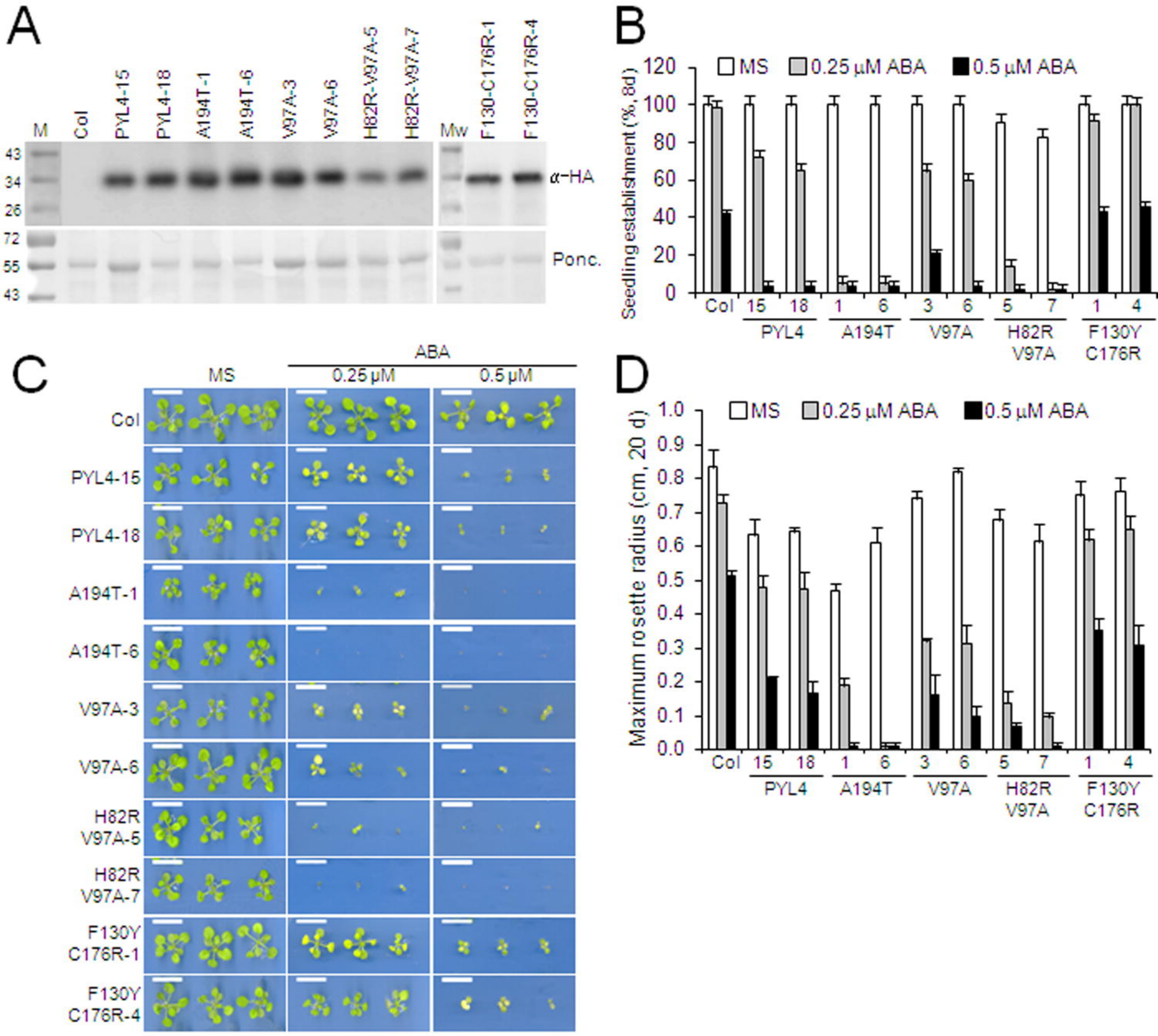
A
M
Col
PYL4-15
PYL4-18
A194T-1
A194T-6
V97A-3
V97A-6
H82R-V97A-5
H82R-V97A-7
Mw
F130-C176R-1
F130-C176R-4
43
34
26
72
55
43
α-HA
Ponc.
B
Seedling establishment (%, 8d)
MS
0.25 μM ABA
0.5 μM ABA
Col
15
18
1
6
3
6
5
7
1
4
PYL4
A194T
V97A
H82R V97A
F130Y C176R
C
ABA
MS
0.25 μM
0.5 μM
Col
PYL4-15
PYL4-18
A194T-1
A194T-6
V97A-3
V97A-6
H82R V97A-5
H82R V97A-7
F130Y C176R-1
F130Y C176R-4
D
Maximum rosette radius (cm, 20 d)
MS
0.25 μM ABA
0.5 μM ABA
Col
15
18
1
6
3
6
5
7
1
4
PYL4
A194T
V97A
H82R V97A
F130Y C176R

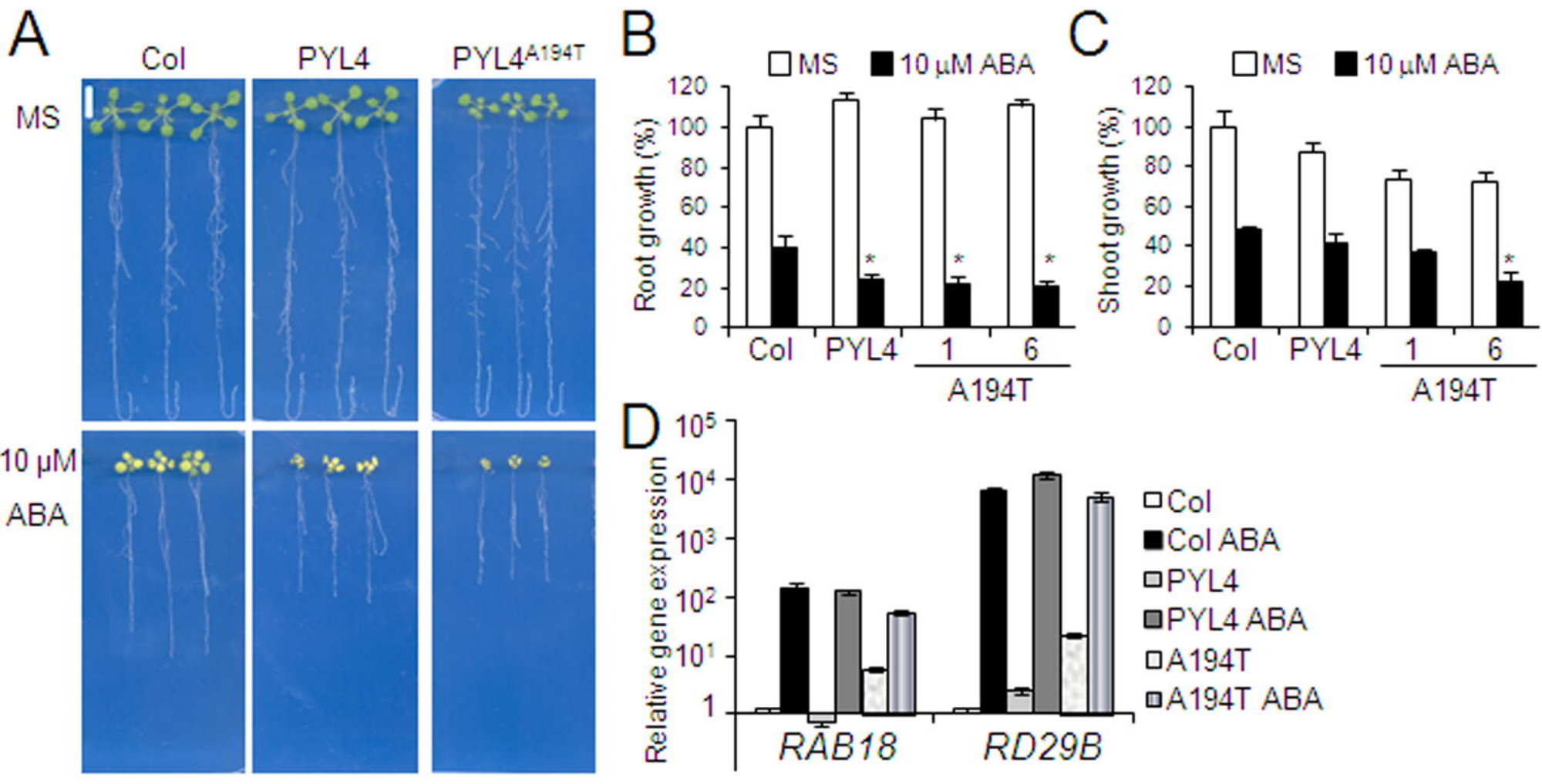
A
Col
PYL4
PYL4A194T
MS
10 µM ABA
B
MS
10 µM ABA
Root growth (%)
120
100
80
60
40
20
0
Col
PYL4
1
6
A194T
C
MS
10 µM ABA
Shoot growth (%)
120
100
80
60
40
20
0
Col
PYL4
1
6
A194T
D
Relative gene expression
10^5
10^4
10^3
10^2
10^1
1
RAB18
RD29B
Col
Col ABA
PYL4
PYL4 ABA
A194T
A194T ABA

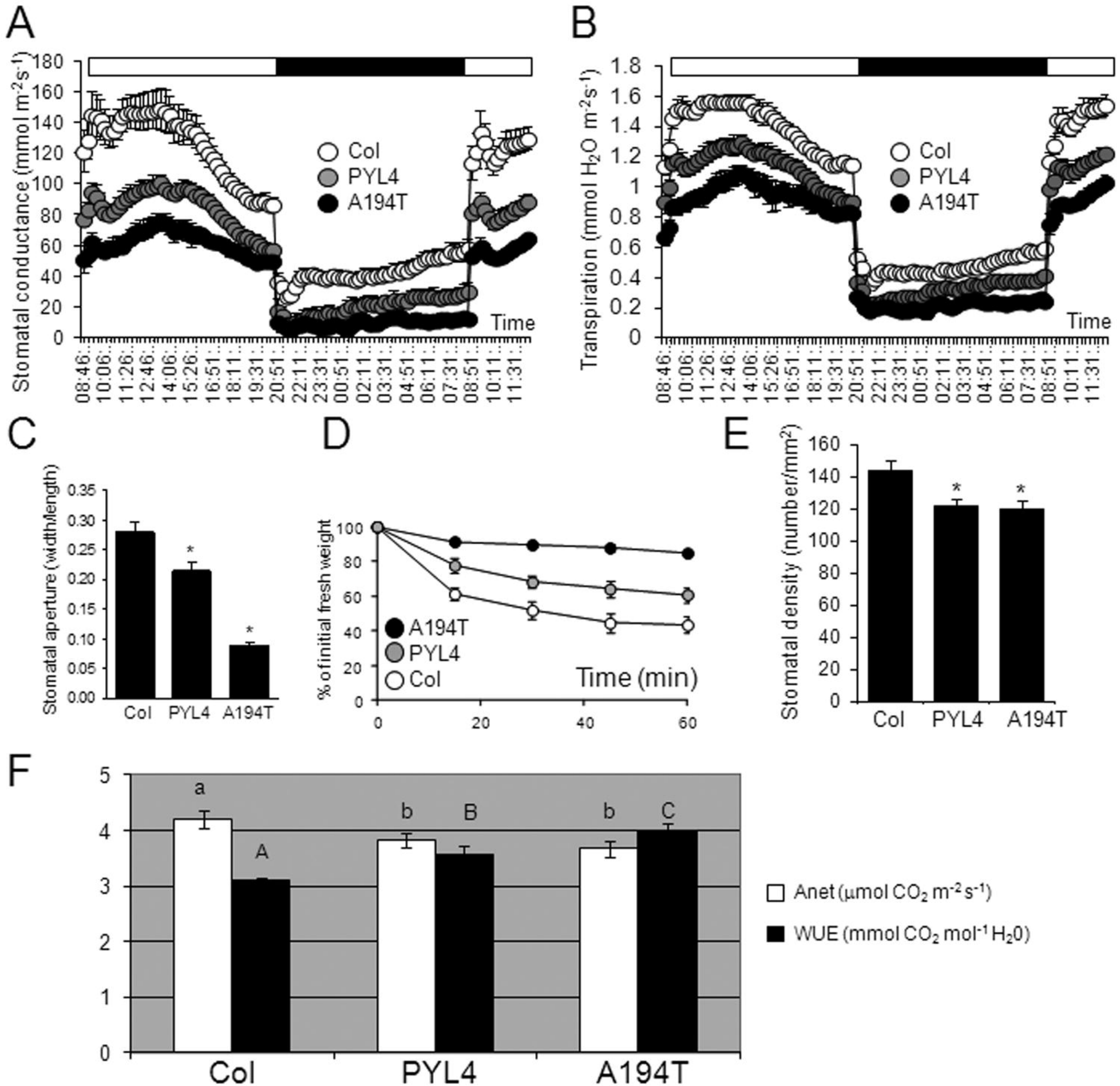
A
Stomatal conductance (mmol m-2s-1)
Col
PYL4
A194T
Time
B
Transpiration (mmol H2O m-2s-1)
Col
PYL4
A194T
Time
C
Stomatal aperture (width/length)
Col
PYL4
A194T
D
% of initial fresh weight
A194T
PYL4
Col
Time (min)
E
Stomatal density (number/mm2)
Col
PYL4
A194T
F
a
A
b
B
b
C
Col
PYL4
A194T
Anet (μmol CO2 m-2 s-1)
WUE (mmol CO2 mol-1 H20)

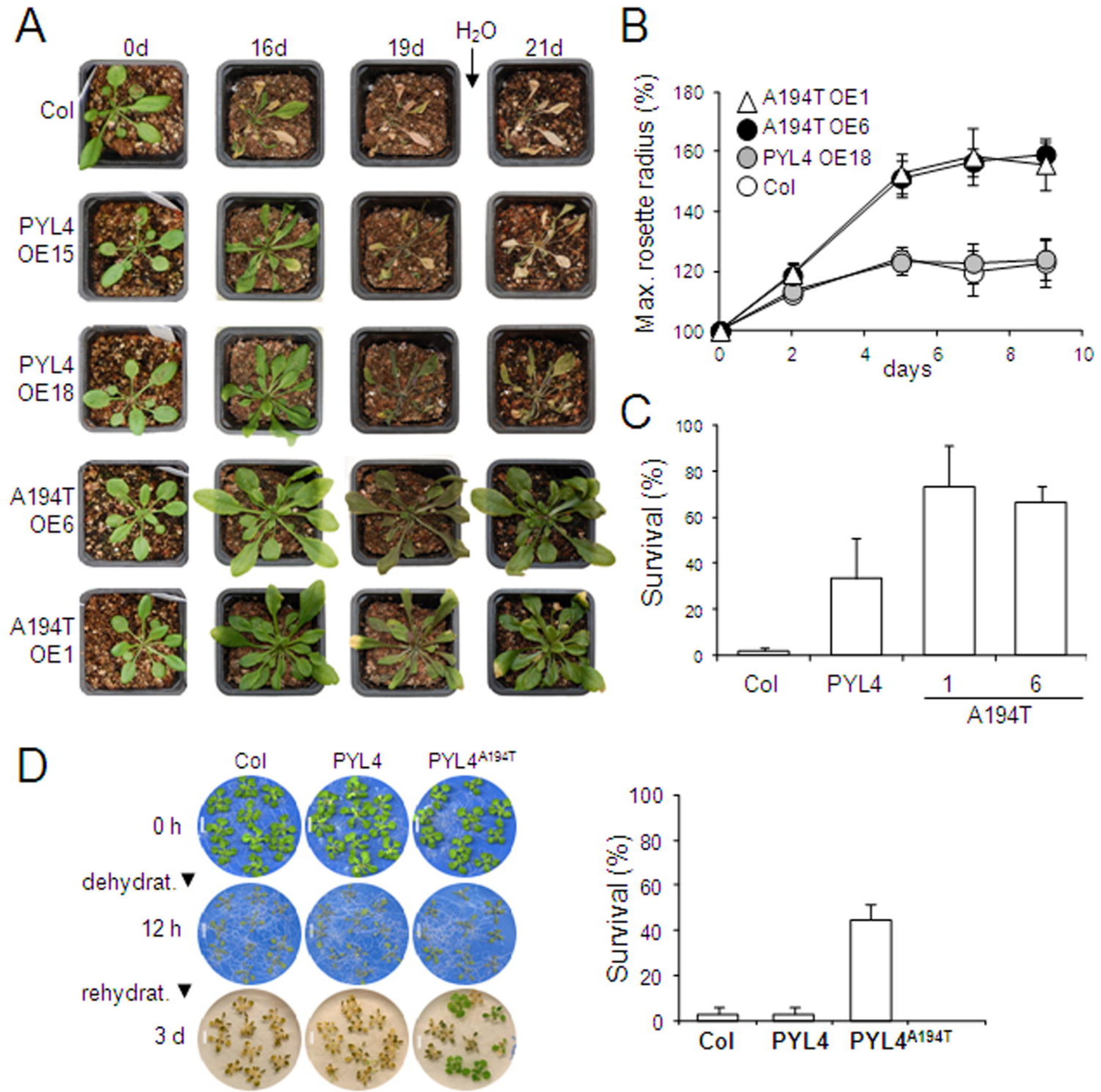
A
0d
16d
19d
H2O
21d
Col
PYL4 OE15
PYL4 OE18
A194T OE6
A194T OE1
B
A194T OE1
A194T OE6
PYL4 OE18
Col
Max. rosette radius (%)
days
C
Survival (%)
Col
PYL4
1
6
A194T
D
Col
PYL4
PYL4A194T
0 h
dehydrat.
12 h
rehydrat.
3 d
Survival (%)
Col
PYL4
PYL4A194T

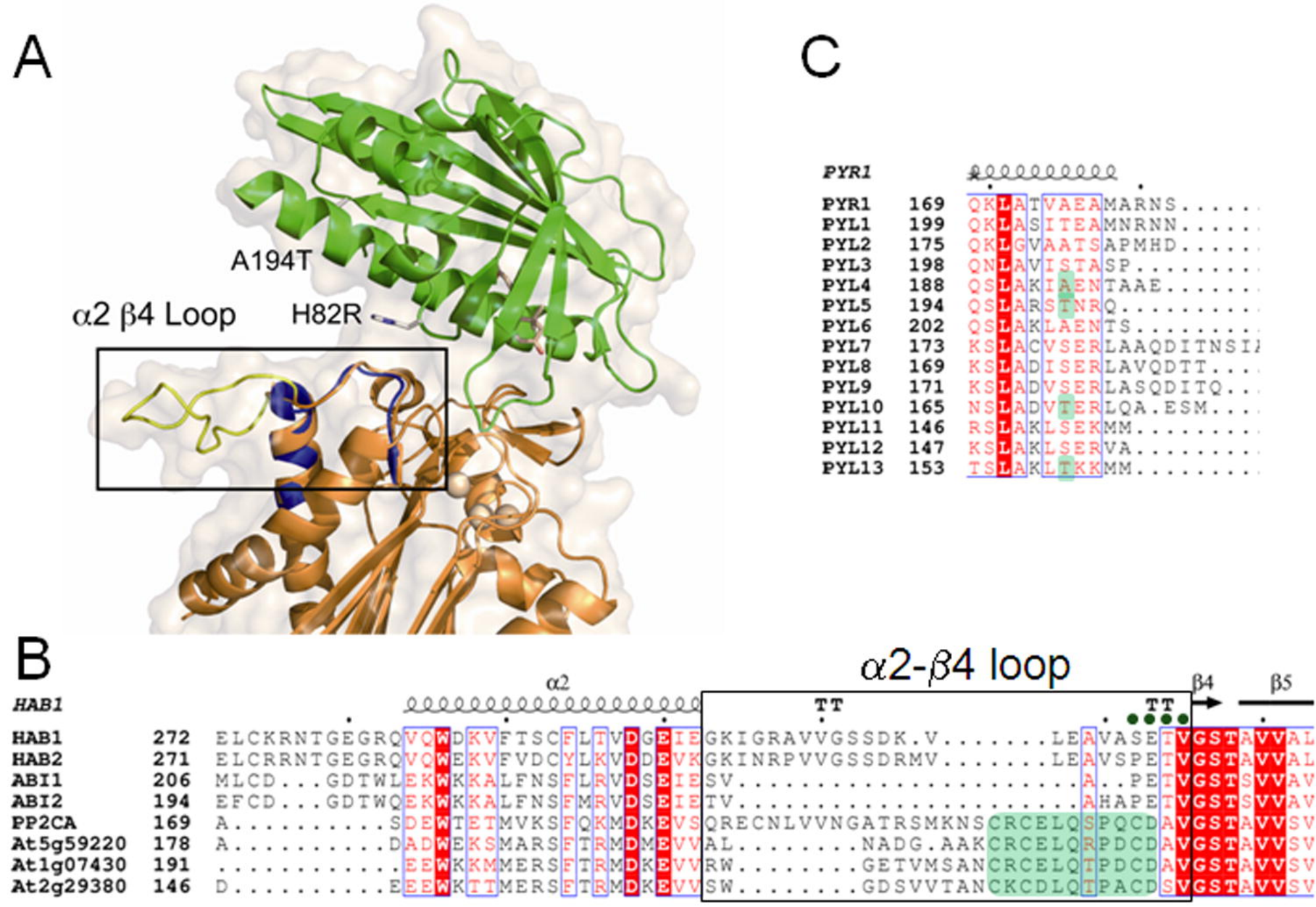
A
A194T
α2 β4 Loop
H82R
C
PYR1
PYR1 169 QKLATVAEAMARNS.....
PYL1 199 QKLASITEAMNRNN.....
PYL2 175 QKLGVAATSAPMHD.....
PYL3 198 QNLAVISTASP.....
PYL4 188 QSLAKIAENTAAE.....
PYL5 194 QSLARSTNRQ.....
PYL6 202 QSLAKLAENTS.....
PYL7 173 KSLACVSERLAAQDITNSI
PYL8 169 KSLADISERLAVQDTT...
PYL9 171 KSLADVSERLASQDITQ..
PYL10 165 NSLADVTERLQA.ESM...
PYL11 146 RSLAKLSEKMM.....
PYL12 147 KSLAKLSERVA.....
PYL13 153 TSLAKLTKKMM.....
B
α2-β4 loop
α2
β4
β5
HAB1
HAB1 272 ELCKRNTGEGRQVQWDKVFTSCFLTVDGEIEGKIGRAVVGSSDK.V.....LEAVASETVGSTAVVAL
HAB2 271 ELCRRNTGEGRQVQWEKVFVDCYLKVDDEVKGKINRPVVGSSDRMV.....LEAVSPETVGSTAVVAL
ABI1 206 MLCD...GDTWLEKWKKALFNSFLRVDSEIESV.....A..PETVGSTSVVAV
ABI2 194 EFCD...GDTWQEKWKKALFNSFMRVDSEIETV.....AHAPETVGSTSVVAV
PP2CA 169 A.....SDEWTETMVKSFQKMDKEVSQRECNLVVNGATRSMKNSCRCELQSPQCDAVGSTAVVSV
At5g59220 178 A.....DADWEKSMARSFTRMDMEVVAL.....NADG.AAKCRCELQRPDCDAVGSTAVVSV
At1g07430 191 .....EEWKKMMERSFTRMDKEVVRW.....GETVMSANCRCELQTPDCDAVGSTAVVSV
At2g29380 146 D.....EEEWKTTMERSFTRMDKEVVSW.....GDSVVTANCKCDLQTPACDSVGSTAVVSV

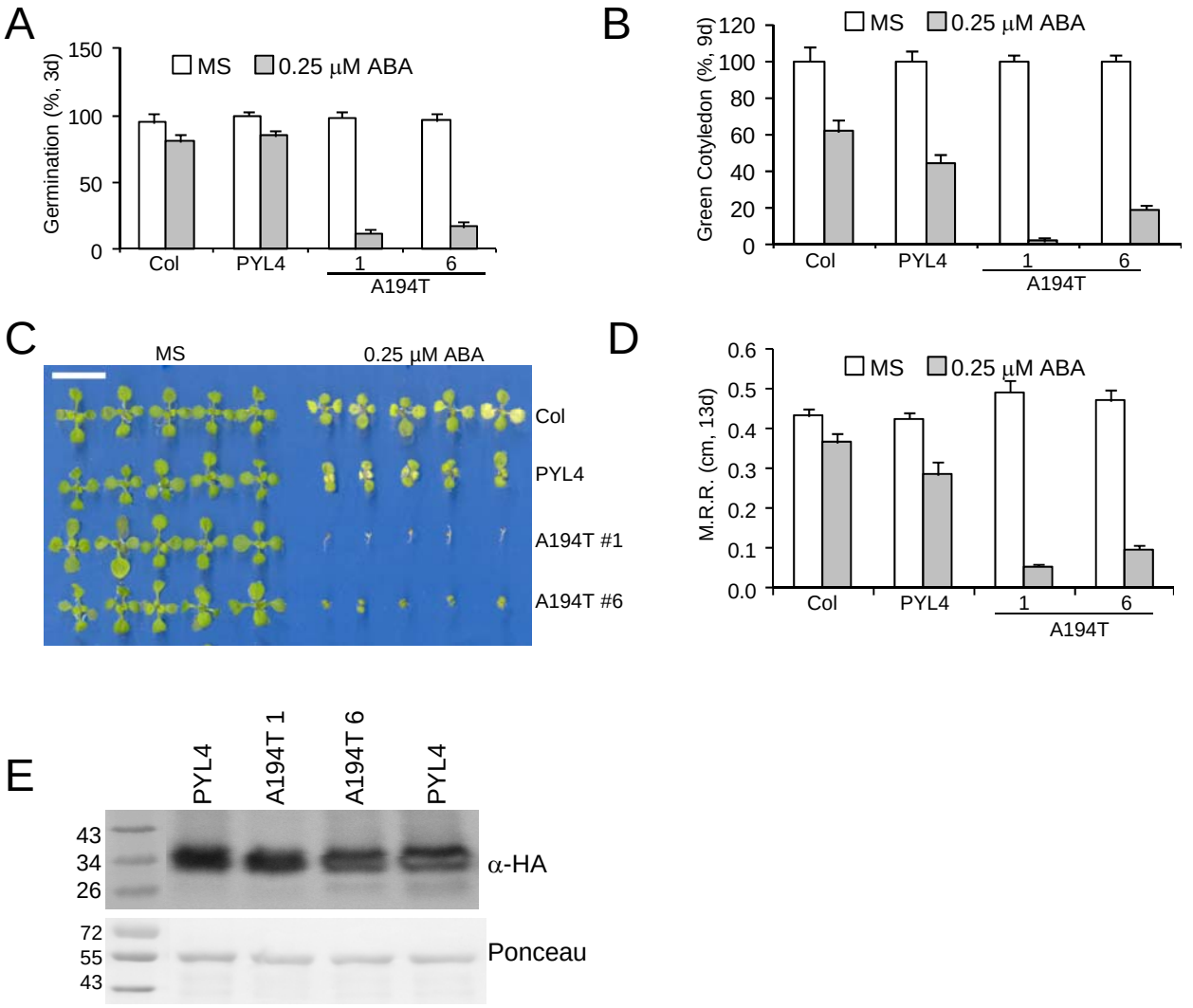

Supplemental Figure S1. Enhanced sensitivity to ABA-mediated inhibition of germination and early seedling growth in T4 PYL4^{A194T} OE plants compared to non-transformed Col and PYL4 OE plants. A, Inhibition of germination (radicle emergence at 3d) and B, seedling establishment (green cotyledons, 9d) by ABA in PYL4^{A194T} OE lines compared to non-transformed Col and PYL4 OE plants. C, The photograph shows enhanced sensitivity to ABA-mediated inhibition of germination and early seedling growth in PYL4^{A194T} OE lines compared to non-transformed Col and PYL4 OE plants. D, Quantification of ABA-mediated early seedling growth inhibition in PYL4 and PYL4^{A194T} OE plants compared to non-transformed Col. Data were obtained by measuring maximum rosette radius (M.R.R.) after 13 d and are averages ± SE from three independent experiments. E, Immunoblot analysis using antibody against HA tag to quantify expression of PYL4 and PYL4^{A194T} in 21-d-old seedlings from T4 transgenic lines. Ponceau staining is shown below as protein loading control.

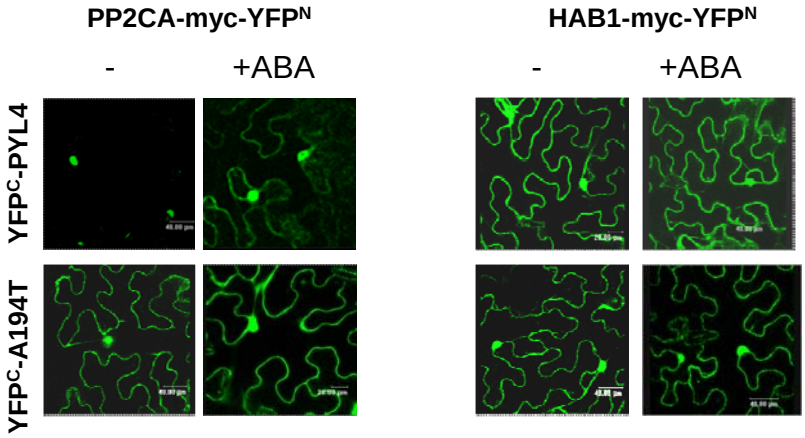

Supplemental Figure S2. ABA infiltration reveals BiFC interaction of PYL4 and PP2CA both at nucleus and cytosol. Laser scanning confocal imaging of epidermal cells infiltrated with a mixture of Agrobacterium suspensions harbouring the indicated BiFC constructs and the silencing suppressor p19. Leaves were examined after 3 days of the infiltration under a Leica TCS-SL confocal microscope. Next, a solution containing 50 mM TrisHCl pH8, 50 μM ABA was injected into leaves that showed BiFC interaction and visualized 1h after injection. A mock injection was performed using 50 mM TrisHCl pH8 buffer.